Rhodospirillum rubrum CO-Dehydrogenase. Part 2. Spectroscopic Investigation and Assignment of Spin−Spin Coupling Signals

Jongyun Heo,[†] Christopher R. Staples,[†] Joshua Telser,[‡] and Paul W. Ludden*,[†]

Contribution from the Department of Biochemistry, College of Agricultural and Life Science, University of Wisconsin-Madison, Madison, Wisconsin 53706, and the Chemistry Program, Roosevelt University, Chicago, Illinois 60605

Received February 8, 1999. Revised Manuscript Received September 10, 1999

Abstract: The carbon monoxide dehydrogenase (CODH) from *Rhodospirillum rubrum* was examined at several potentials. The electron paramagnetic resonance (EPR) spectrum of CODH poised at approximately −295 mV exhibits a species (referred to as C_{red1}) that was previously attributed to $[Fe_4S_4]_C^{1+}$ ($S = 1/2$) weakly exchange-coupling with Ni^{2+} ($S = 1$) to yield apparent g-values of ($g_{z,y,x} = 2.03, 1.88, 1.71$). UV−visible absorption spectroscopy showed only one $[Fe_4S_4]$ cluster to be reduced at −295 mV. Based upon our assignment of $S = 1/2$ resonances in indigo carmine-poised C531A CODH (see Part 1: Staples, C. R.; Heo, J.; Spangler, N. J.; Kerby, R. L.; Roberts, G. P.; Ludden, P. W. *J. Am. Chem. Soc.* In press) to a $[(CO_L)Fe^{3+}\text{-}Ni^{2+}\text{-}H^-]^{4+}$ cluster, a careful search for similar resonances in the EPR spectrum of the enzyme state of wild-type CODH producing C_{red1} was undertaken. Coupled putative $[(CO_L)Fe^{3+}\text{-}Ni^{2+}\text{-}H^-]^{4+}$ signals were observed in low intensity, which, in conjunction with the other assignments, prompted a reinterpretation of the redox state of the enzyme producing C_{red1}. Instead of coupling with Ni^{2+} ($S = 1$), we propose $[Fe_4S_4]_C^{1+}$ ($S = 1/2$) couples with $[(CO_L)\text{-}Fe^{3+}\text{-}Ni^{2+}\text{-}H^-]^{4+}$ ($S = 1/2$). The putative [FeNi] signals were heterogeneous, but this heterogeneity could be removed by preincubation with CO prior to subsequent poising. We propose that an unreactive CO molecule (CO_L) is bound to the [FeNi] cluster, possibly modulating the reduction potential and activating the [FeNi] cluster for catalysis of a substrate CO molecule (CO_S). Either Zn^{2+} or Co^{2+} was incorporated into purified, Ni-deficient CODH. The EPR spectra of reduced Zn-CODH and Co-CODH contain resonances in the $g =$ 1.73−1.76 region (which we call C_{red2A}), and an upfield wing (shoulder) near $g = 2.09$. That these features are observed without a paramagnetic heterometal present indicates that they are derived solely from the $[Fe_4S_4]^{1+}$ clusters. These resonances are attributed in fully reduced CODH to spin−spin coupling between $[Fe_4S_4]_C^{1+}$ ($S = 1/2$) and $[Fe_4S_4]_B^{1+}$ ($S = 1/2$). When CODH was poised at a calculated potential of −326 mV, the UV−visible absorption spectrum indicated that only one of the $[Fe_4S_4]$ clusters was reduced. However, the EPR spectrum was much different than that observed at ca. −295 mV. The EPR spectrum of CODH at −326 mV exhibited resonances arising from a slow-relaxing $[Fe_4S_4]^{1+}$ ($S = 1/2$) cluster ($g_{z,y,x} = 2.04, 1.93, 1.89$) and a very minor amount of a fast-relaxing $[Fe_4S_4]^{1+}$ ($S = 1/2$) cluster. None of the C_{red1} coupling signal was present. The fast-relaxing cluster is assigned to $[Fe_4S_4]_B^{1+}$, while the slow-relaxing cluster is assigned to uncoupled $[Fe_4S_4]_C^{1+}$. The observation of uncoupled $[Fe_4S_4]_C^{1+}$ at slightly lower potentials suggests the reduction of $[(CO_L)Fe^{3+}\text{-}Ni^{2+}\text{-}H^-]^{4+}$ ($S = 1/2$) to $[(CO_L)Fe^{2+}\text{-}Ni^{2+}\text{-}H^-]^{3+}$ ($S = 0$). Treatment of CODH with its physiological product (CO_2) while poised at −326 mV with 99% reduced phenosafranin results in accumulation of oxidized dye, the production of CO, and the appearance of a new species with $g_x = 1.75$. This species has relaxation properties unlike C_{red2A}. Based upon the method of generation and the relaxation properties of the species, the $g = 1.75$ feature is assigned to $[Fe_4S_4]_C^{1+}$ ($S = 1/2$) spin-coupling with $[Fe^{2+}\text{-}Ni^{2+}]^{4+}$ ($S = 1$) (and is referred to as C_{red2B}). Based on the data presented in this and Part 1, a mechanism for the oxidation of CO to CO_2 by *R. rubrum* CODH is proposed.

Introduction

Carbon monoxide dehydrogenase (CODH) catalyzes the two-electron oxidation of CO to CO_2, with the concurrent production of protons, according to the following reaction:

$$CO + H_2O \rightleftarrows CO_2 + 2e^- + 2H^+$$

This transformation occurs on the enzyme at a location referred to as the C-site. CODHs from both *Clostridium thermoaceticum* and *Rhodospirillum rubrum* contain the C-site, which has been shown to encompass both an $[Fe_4S_4]$ cluster and a nickel species (ref 1 and references therein).[1] For the sake of clarity, the $[Fe_4S_4]$ cluster at the C-site will be referred to as $[Fe_4S_4]_C$. In addition to the C-site, *R. rubrum* contains another cluster referred to as the B-site. All research thus far[2,3] has shown the B-site cluster to have properties consistent with an all-cysteinyl liganded $[Fe_4S_4]$ cluster (referred to as $[Fe_4S_4]_B$

* Address correspondence to this author.
[†] University of Wisconsin-Madison.
[‡] Roosevelt University.

(1) Hu, Z.; Spangler, N. J.; Anderson, M. E.; Xia, J.; Ludden, P. W.; Lindahl, P. A.; Münck, E. *J. Am. Chem. Soc.* **1996**, *118*, 830−845.
(2) Lindahl, P. A.; Ragsdale, S. W.; Münck, E. *J. Biol. Chem.* **1990**, *265*, 3880−3888.
(3) Lindahl, P. A.; Münck, E.; Ragsdale, S. W. *J. Biol. Chem.* **1990**, *265*, 3873−3879.

10.1021/ja990397a CCC: $18.00
Published on Web 11/18/1999

hereafter). The *C. thermoaceticum* CODH also contains a site of acetyl-CoA synthase activity, termed the A-site, the properties of which have been demonstrated to be quite similar to the C-site. [2,4−7]

Research concerning the exact mechanism of CO oxidation has thus far been hindered by confusion about the redox states of the metal centers. This confusion has been due in large part to unusual resonances observable by electron paramagnetic resonance (EPR) spectroscopy. Several proposed mechanisms have required the inclusion of a redox-active ligand or EPR silent intermediates to reconcile the postulated metal redox states producing the EPR signals with the necessary flow of electrons out of the C-site. These have included proposed unobservable X, S, or C_{int} species and redox states.[5,8,9]

Enigmatic EPR resonances exhibited by CODH are referred to as C_{red1} and C_{red2}. C_{red1} has apparent *g*-values at $g = 2.03$, 1.88, and 1.71 in *R. rubrum*, and has been postulated to arise from the redox state of the C-site which binds CO.[5,9] The EPR spectrum of C_{red1} is variably broadened by both ^{57}Fe and ^{61}Ni in *R. rubrum* CODH,[10] and therefore the system was proposed to involve the weak exchange-coupling of Ni^{2+} ($S = 1$) and $[Fe_4S_4]^{1+}$ ($S = 1/2$) to yield a $[Fe_4S_4]^{1+}$ cluster with a perturbed $S = 1/2$ state.[1] After substrate binding, two electrons were proposed to enter the C-site, producing C_{red2}.[5] The C_{red2} signal can be seen in fully (dithionite) reduced Ni-CODH (defined as CODH with Ni present; either as-purified from Ni-containing medium, or as-purified in a Ni-deficient form from medium devoid of Ni, and subsequently reconstituted with Ni) and in CODH titrated with CO. Only the g_x principal *g*-value of C_{red2} in dithionite-treated CODH has been directly observed ($g_x \sim 1.75$), while the g_z and g_y values have been simulated to be positioned at $g_z = 1.97$ and $g_y = 1.87$, their positions in CO-treated CODH.[1]

CO-induced CODH *R. rubrum* enzyme can be purified in an inactive, Ni-deficient form.[11−13] This Ni-deficient CODH contains two $[Fe_4S_4]$ clusters whose relaxation properties, as monitored by EPR, differ as a function of temperature. Ni-deficient CODH is able to be fully activated to the levels of Ni-CODH by incubation with nickel in a 100% CO atmosphere, suggesting that Ni-deficient CODH has a similar structure to that of Ni-CODH, but lacks only the nickel.[11] Metals other than nickel can be inserted into Ni-deficient CODH, and after insertion, the enzyme has very low or background activity that cannot be increased by incubation with nickel. Thus, once inserted, the heterometal is not easily removed. While the Zn- and Co-inserted forms of Ni-deficient CODH (referred to as Zn-CODH and Co-CODH, respectively) have been produced previously, until now they have not been fully characterized by spectroscopic methods. We make use of Zn-CODH and Co-CODH, in conjunction with our knowledge of the presence of a putative $[(CO_L)Fe-Ni]$ cluster in Ni-CODH (as described in the Part 1), to determine the origins of the C_{red} coupling signals. Based on the data presented in this paper and Part 1, a mechanism for the oxidation of CO to CO_2 by *R. rubrum* CODH is proposed.

Experimental Procedures

Cell Growth and Protein Purification. Wild-type *R. rubrum* Strain UR2 was cultured and CODH was purified as described previously,[11−14] and as described in Part 1 for C531A CODH. Ni-deficient CODH was purified according to previously published methods.[11−14] The purified Ni-deficient CODH had a specific activity of 0.5 unit/mg, compared to 7000−10000 units/mg for Ni−CODH. All buffers used in purification of, and incorporation of Co^{2+} and Zn^{2+} into, Ni-deficient CODH from nickel-depleted cultures were passed over a metal chelating column of Bio-Rad Chelex-100 cation-exchange resin. All the vials were soaked in 1.0 N HCl for a day, rinsed with metal-free chelexed 100 mM MOPS buffer, and stored in an anaerobic atmosphere (Vacuum/Atmospheres Dri-Lab glovebox, Model HE-493) containing less than 2 ppm of oxygen.

Assays. The CO-dehydrogenase activity, metal analyses, and protein assays were determined as described in Part 1.

Sample Manipulations. All manipulations were performed in an anaerobic glovebox (Vacuum Atmospheres) under an atmosphere containing less than 2 ppm O_2.

Preparation of CODH for UV−Visible Absorption Spectroscopy of the Enzyme State Producing C_{red1}. Purified CODH in buffer containing 2 mM dithionite was passed down a Sephadex G-25 column equilibrated in 10 mM MOPS buffer at pH 7.5 to remove excess dithionite. For preparation of CODH in oxidized states or partially reduced states, the enzyme was then treated with either an excess of thionin ($E_m = +64$ mV versus SHE) or 95% reduced 2-hydroxy-1,4-naphthoquinone ($E_m = -257$ mV versus SHE at pH 8.5; calculated *E* when 95% reduced $= -295$ mV versus SHE), respectively. 2-Hydroxy-1,4-naphthoquinone was determined to be 95% reduced by monitoring the absorption and titrating with ultrapure sodium dithionite. The dyes and salt were subsequently removed from CODH by passage of the enzyme through a 0.5 × 10 cm Sephadex G-25 column equilibrated with 100 mM Tris−HCl buffer. The CODH solution was transferred to quartz cuvettes which were sealed with rubber serum stoppers before bringing the samples out of the glovebox for UV−visible spectral measurements. Enzyme pretreated with either dye was subsequently titrated with a 1 mM sodium dithionite solution until the first appearance of the characteristic dithionite absorption at 314 nm. The dithionite solution was added via gastight syringe through the serum stopper. Spectra were also recorded for samples treated with a large excess of dithionite to ensure that all species reducible by dithionite were fully reduced. Where indicated, CO was introduced via gastight syringe into the headspace of stoppered quartz cuvettes containing enzyme. The enzyme was incubated under CO at room temperature for 5 min, and the spectrum was recorded. Identical samples were prepared for EPR analysis. Molar absorption coefficients were obtained as described in Part 1.

Preparation of CODH for EPR Spectroscopy of the Enzyme State Producing C_{red1}. Purified wild-type *R. rubrum* CODH in 2 mM dithionite was passed down a Sephadex G-25 column equilibrated in 10 mM MOPS buffer at pH 7.5 to remove excess dithionite. Most protein concentrations were 10 mg/mL. Both as-isolated CODH and a CO preincubated CODH (20 min) were oxidized individually by a slight excess of thionin ($E_m = +56$ mV),[15] which was subsequently removed by passage down a 0.5 × 25 cm Sephadex G-25 column equilibrated in 10 mM MOPS buffer (pH 7.5 or 8.5). The enzyme was incubated with a large excess of 95% reduced 2-hydroxy-1,4-naphthoquinone (pH 8.5) for 5 min before freezing in the EPR tube.

Incorporation of Co^{2+} and Zn^{2+} into Ni-Deficient CODH (Preparation for EPR Spectroscopy of the Enzyme State Producing C_{red2A}). Ni-deficient CODH (5 mg) was bound to a 0.50 × 1 cm column

(4) Kumar, M.; Lu, W.-P.; Ragsdale, S. W. *Biochemistry* **1994**, *33*, 9769−9777.
(5) Seravalli, J.; Kumar, M.; Lu, W.-P.; Ragsdale, S. W. *Biochemistry* **1995**, *34*, 7879−7888.
(6) Shin, W.; Lindahl, P. A. *J. Am. Chem. Soc.* **1992**, *114*, 9718−9719.
(7) Anderson, M. E.; Lindahl, P. A. *Biochemistry* **1994**, *33*, 8702−8711.
(8) Seravalli, J.; Kumar, M.; Lu, W.-P.; Ragsdale, S. W. *Biochemistry* **1997**, *36*, 11241−11251.
(9) Anderson, M. E.; Lindahl, P. A. *Biochemistry* **1996**, *35*, 8371−8380.
(10) Stephens, P. J.; McKenna, M.-C.; Ensign, S. A.; Bonam, D.; Ludden, P. W. *J. Biol. Chem.* **1989**, *264*, 16347−16350.
(11) Bonam, D.; McKenna, M. C.; Stephens, P. J.; Ludden, P. W. *Proc. Natl. Acad. Sci. U.S.A.* **1988**, *85*, 31−35.
(12) Ensign, S. A.; Bonam, D.; Ludden, P. W. *Biochemistry* **1989**, *28*, 4968−4973.
(13) Ensign, S. A.; Campbell, M. J.; Ludden, P. W. *Biochemistry* **1990**, *29*, 2162−2168.
(14) Bonam, D.; Murrell, S. A.; Ludden, P. W. *J. Bacteriol.* **1984**, *159*, 693−699.
(15) Lu, W. P.; Jablonski, P. E.; Rasche, M.; Ferry, J. G.; Ragsdale, S. W. *J. Biol. Chem.* **1994**, *269*, 9736−9742.

of DE-52 anion-exchange resin (Whatman) equilibrated with 100 mM MOPS buffer (pH 7.5) containing 0.20 mM dithionite in a Vacuum Atmospheres glovebox containing less than 2 ppm O_2. Column-bound Ni-deficient CODH was treated with 10 mL of 5.0 mM $CoCl_2$ or $ZnCl_2$ in 100 mM MOPS, 0.20 mM dithionite, and 0.20 mM methyl viologen at pH 7.5; the Co^{2+}- or Zn^{2+}-containing solution was passed through the column at a flow rate of 0.10 mL/min.[12] Excess $CoCl_2$ and $ZnCl_2$ was removed by washing with 100 mL of 100 mM MOPS buffer containing 0.10 mM dithionite, and 0.10 mM EDTA. The protein was eluted with 400 mM NaCl in 100 mM MOPS buffer containing 1 mM dithionite, then desalted by passage down a 0.50 × 10 cm Sephadex G-25 column with 100 mM MOPS buffer containing 1.0 mM dithionite.

Preparation of CODH for UV−Visible Absorption Spectroscopy of the Enzyme State Producing C_{red2B}. Purified wild-type *R. rubrum* CODH in 2 mM dithionite was passed down a Sephadex G-25 column equilibrated in 10 mM MOPS buffer at pH 7.5 to remove excess dithionite. The enzyme was then oxidized by a slight excess of thionin ($E_m = +64$ mV),[15] which was subsequently removed by passage down a 0.5 × 25 cm Sephadex G-25 column equilibrated in 10 mM MOPS buffer (pH 7.5 or 8.5). The eluent (0.014 mM CODH) was sealed anaerobically in quartz cuvettes for UV−visible spectral studies. To the sealed cuvette was added 99% reduced phenosafranin (0.5 mM) and the spectrum was monitored from 200 to 900 nm. Phenosafranin was determined to be 99% reduced by monitoring the absorption and titrating with ultrapure (sodium bicarbonate-free) sodium dithionite. Sodium bicarbonate was added as indicated and the enzyme was incubated for 10 min. Finally, changes in the spectra were monitored. Sodium bicarbonate was prepared in 1 M MOPS buffer (pH 7.5) to avoid changing the pH of the final solution when added. Molar absorption coefficients were obtained as described in Part 1.

Preparation of CODH for EPR Spectroscopy To Observe C_{red2B}. CODH (0.2 mM) used for EPR samples was oxidized by thionin, which was subsequently removed by gel filtration. The enzyme was then poised with phenosafranin (1.0 M, 99% reduced by dithionite) for 5 min. Where indicated, after poising with phenosafranin, the enzyme was treated with either 400 mM NaCl, 50% poly(ethyleneglycol) (4000 MW_{ave}), or 10 mM $NaHCO_3$ for 10 min to allow for equilibration.

UV−Visible and EPR Spectroscopy Instrumentation. The equipment used for spectral measurements is described in Part 1.

Materials. Materials used are described in Part 1, with the exception of 2-hydroxy-1,4-naphthoquinone (97%), which was obtained from Aldrich, sodium bicarbonate ($NaHCO_3$), which was obtained from Fisher Scientific, and phenosafranin (80%), which was obtained from Aldrich.

Results

Characterization of the Enzyme State Producing C_{red1}. (a) UV−Visible Spectroscopy of CODH Poised at Different Potentials. To determine the redox states of the $[Fe_4S_4]$ clusters of CODH at different potentials, the UV−visible absorption spectra were obtained (as shown in Figure 1) for (i) thionin-oxidized, (ii) 2-hydroxy-1,4-naphthoquinone-poised, (iii) dithionite-treated, and (iv) CO-reduced CODH. The inset shows the spectra of thionin-oxidized (upper trace) and quinone-poised (lower trace) CODH minus dithionite-reduced CODH. Upon quinone treatment, the absorbance at 420 (ϵ_{420}) decreases by 50% of the decrease that occurs upon dithionite treatment. This, in conjunction with the EPR results presented below, establishes that only one of the two $[Fe_4S_4]$ clusters is reduced at this potential (−295 mV). The decrease in absorption from the thionin-oxidized form of CODH indicates that this single $[Fe_4S_4]$ cluster is fully reduced at −295 mV.

(b) EPR Spectroscopy of CODH Poised in the State Producing C_{red1}. To correlate the EPR spectroscopic states of CODH with the absorption of CODH, EPR spectra were obtained for samples poised at the same potentials as described in Figure 1. Figure 2A shows the temperature dependency at 1.0 mW power of the $g = 2$ region of the EPR spectrum of *R. rubrum* CODH poised with 95% reduced 2-hydroxy-1,4-naphthoquinone at pH 8.5 ($E_m = -257$ mV versus SHE at pH 8.5; calculated E when 95% reduced = −295 mV versus SHE). The signal referred to as C_{red1} (simulated $g_{z,y,x} = 2.03, 1.88, 1.71$) is in excellent agreement to those previously reported for *R. rubrum* CODH[1] (e.g. the spectrum recorded at 15 K in Figure 2A), with optimum intensity at 1.0 mW determined to be at ∼12 K (Figure 2B), based upon the intensity of the $g = 1.71$ resonance. Also observed are numerous resonances at lower field than $g = 2.03$ (shown in an expanded form in later figures); these will be discussed below. At higher temperatures, unusual resonances at $g = 2.02$ and 1.94 remain observable. The 2.02 feature is similar in line shape and g-values to $[Fe_3S_4]^{1+}$ clusters which are weakly coupled to another $S = 1/2$ paramagnet.[16] Our working hypothesis is it represents a small fraction of a

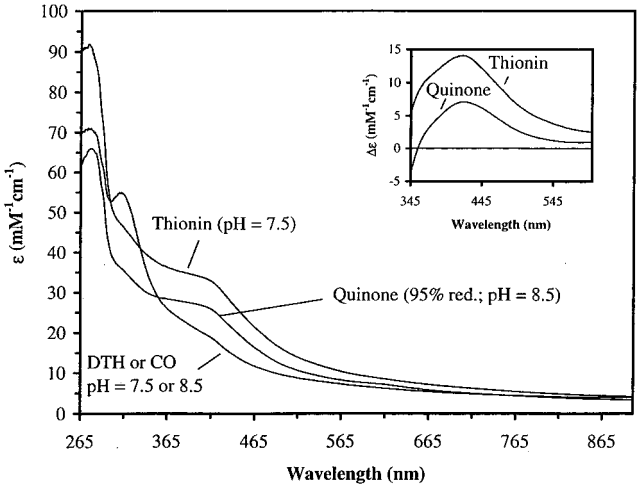

Figure 1. UV−visible absorption spectra of wild-type CODH treated with thionin (+128 mV), 95% reduced 2-hydroxy-1,4-naphthoquinone at pH 8.5 (−295 mV), CO, or dithionite. Inset: Difference spectra of thionin-oxidized (upper trace) and 95% reduced 2-hydroxy-1,4-naphthoquinone-treated CODH (lower trace) minus dithionite-treated CODH.

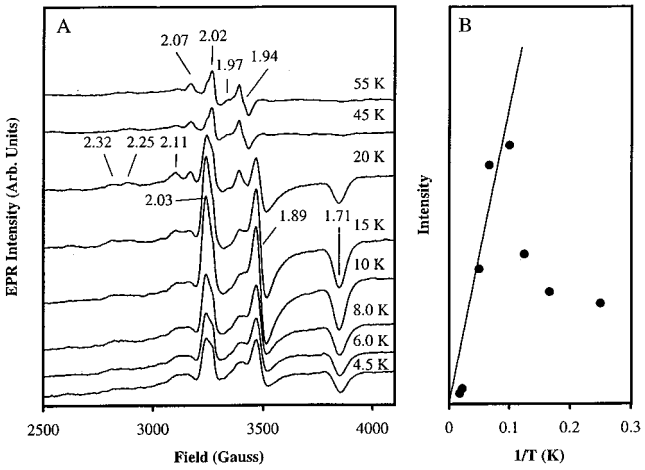

Figure 2. X-band EPR temperature study of the $g = 2$ region of *R. rubrum* CODH poised with 95% reduced 2-hydroxy-1,4-naphthoquinone. Left panel (A): EPR spectra using microwave frequency = 9.23 GHz, microwave power = 1.0 mW, modulation amplitude = 10 G, modulation frequency = 100 kHz, and time constant = 1 s. Spectra are each the sum of 4 scans, with a 4 scan cavity background subtracted. Right panel (B): Plot of the intensity of the $g = 1.71$ feature versus reciprocal temperature.

(16) Surerus, K. K.; Chen, M.; Van der Zwaan, W. J.; Rusnak, F. M.; Kolk, M.; Duin, E. C.; Albracht, S. P. J.; Munck, E. *Biochemistry* **1994**, *33*, 4980−4993.

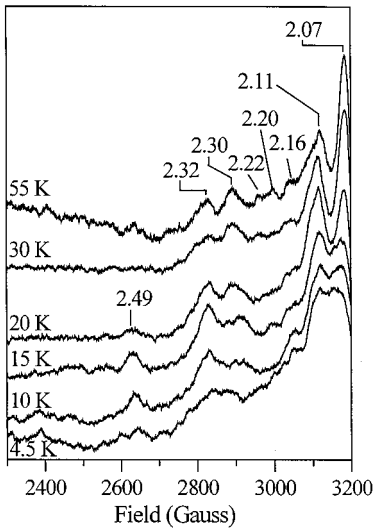

Figure 3. X-band EPR temperature study of the $g > 2.03$ resonances in the $g = 2$ region of *R. rubrum* CODH poised as in Figures 1 and 2. EPR conditions: microwave frequency = 9.23 GHz, microwave power = 1.0 mW, modulation amplitude = 10 G, modulation frequency = 100 kHz, time constant = 1 s. Spectra are each the sum of 12 scans, with a 12 scan cavity background subtracted.

$[Fe_3S_4]_C^{1+}$ species (arising from degraded $[Fe_4S_4]_C$) that is coupled to the $g_{ave} = 2.16$ resonance described below. In addition to the $g = 2.02$ feature, the $g_{ave} = 2.16$ signal, the C_{red1} signal, and a derivative at $g = 1.94$ are present in low intensity at 55 K. Also present is a $g = 2.07$ resonance (shown more clearly in Figure 3), but whether this is the principle g_z-value of the $g = 1.94$ derivative is not clear at this time. At 12 K, power-saturation begins to become apparent above 4.0 mW, as determined by the intensity of the $g = 1.71$ resonance (not shown). These observations are important in that C_{red1} is often reported for samples at 10 K, with powers ranging from 40 to 80 mW, i.e., saturating conditions. The total spin-integration of the entire $g \cong 2$ region from $g = 2.40$ to 1.60 equates to 0.20 ± 0.03 spins/molecule. However, signals arising from more than one species are present in the $g \sim 2$ region of the EPR spectrum when CODH is poised with naphthoquinone. The data presented below will be interpreted as evidence that the other signal does not arise from a $[Fe_4S_4]$ cluster and does not contribute intensity to the ϵ_{420} of the UV−visible spectrum.

(c) Evidence for EPR Signals Attributable to a [FeNi] Cluster in Wild-type CODH. The region of the EPR spectrum containing resonances from the species not attributed to a $[Fe_4S_4]^{1+}$ cluster is described in this section. Figure 3 shows a temperature study at 1.0 mW of the narrow range of the EPR spectrum containing the resonances at $g > 2.03$ observed in the same sample shown in Figure 2. Several features with slightly differing relaxation properties can be observed in this region. The intensity of most features is maximum at around 15 K, as are the features that comprise C_{red1}. Most features have a qualitative optimal power for observation of undistorted signals similar to the features typically referred to as C_{red1} (not shown). At powers above 5.0 mW, the features in the $g > 2.03$ region are severely distorted and broadened. With the exception of the $g = 2.49$ and 2.07 features, the g-values and line shapes of the majority species in the $g > 2.03$ region of 2-hydroxy-1,4-naphthoquinone-poised wild-type CODH and the $g_{ave} = 2.16$ signal in C531A CODH are very similar. The qualitative power saturation behavior and temperature dependency of the signal intensity (Figure 3, and refer to Part 1) of the resonances in wild-type and C531A CODH's are also similar. In C531A CODH these resonances have been postulated to arise from a $[(CO_L)Fe^{3+}\text{-}Ni^{2+}\text{-}H^-]^{4+}$ ($S = 1/2$) species (CO_L = nonsubstrate CO ligand to the [FeNi] cluster). A decrease in absorbance of CODH at 420 nm upon 2-hydroxy-1,4-naphthoquinone treatment which is only 50% of the decrease in absorbance when treated with dithionite indicates that only one $[Fe_4S_4]$ cluster is reduced. Because the $[Fe_4S_4]_B^{2+/1+}$ couple occurs at $E_m = -415$ mV versus SHE,[1,17] we propose that only $[Fe_4S_4]_C$ is reduced at −295 mV. However, there are at least two species in the EPR spectrum upon 2-hydroxy-1,4-naphthoquinone treatment, one of which resembles the $g_{ave} = 2.16$ species in C531A CODH. The $g_{ave} = 2.16$ species is produced in C531A CODH, without a concurrent decrease in absorbance, by treatment with 95% reduced indigo carmine. Thus the $g > 2.03$ species in wild-type CODH is probably also produced without a concurrent decrease in absorbance. The similar properties of the $g > 2.03$ features in 2-hydroxy-1,4-naphthoquinone poised wild-type CODH compel us to assign the majority of them to the $[(CO_L)Fe^{3+}\text{-}Ni^{2+}\text{-}H^-]^{4+}$ species ($g_{ave} = 2.16$) seen in C531A CODH. The assignment of the $g > 2.03$ resonances to the $[(CO_L)Fe^{3+}\text{-}Ni^{2+}\text{-}H^-]^{4+}$ species ($g_{ave} = 2.16$) seen in C531A CODH instigated a reassessment of the interpretation of enzyme state producing C_{red1} in *R. rubrum* CODH. The following section will describe a proposal that C_{red1} is the result of the coupling of $[Fe_4S_4]_C^{1+}$ ($S = 1/2$) with $[(CO_L)Fe^{3+}\text{-}Ni^{2+}\text{-}H^-]^{4+}$ ($S = 1/2$), rather than Ni^{2+} ($S = 1$) as was previously believed.

(d) The Enzyme State of CODH Producing C_{red1} Is the Result of the Coupling of $[(CO_L)Fe^{3+}\text{-}Ni^{2+}\text{-}H^-]^{4+}$ ($S = 1/2$) with $[Fe_4S_4]_C^{1+}$ ($S = 1/2$). In Part 1 it was proposed that the $g_{ave} = 2.16$ signal in C531A CODH arises from a $[(CO_L)Fe^{3+}\text{-}Ni^{2+}\text{-}H^-]^{4+}$ species that is produced upon reduction of the oxidized enzyme. The $g_{ave} = 2.16$ signal is not present in thionin-oxidized wild-type CODH, but can be observed at −295 mV in low spin quantity. Thus, similarly to C531A CODH, a putative $[(CO_L)Fe^{2+}\text{-}Ni^{2+}]^{4+}/[(CO_L)Fe^{3+}\text{-}Ni^{2+}\text{-}H^-]^{4+}$ transition can occur in wild-type CODH. Future sections will demonstrate that the $g_{z,y,x} = 2.03, 1.88, 1.71$ signal shifts to a $g_{z,y,x} = 2.04, 1.93, 1.89$ signal upon a change in potential from −295 to −326 mV, while the ϵ_{420} of the UV−visible spectrum is unchanged. At the lower potential, the spin quantitation of the $g = 2$ region increases to 0.65 ± 0.05 spins/molecule from 0.20 ± 0.03 spins/molecule at $E = -295$ mV. The total spin intensity of dithionite-reduced CODH (WT, Co-CODH, or Zn-CODH) is $\sim 1.50 \pm 0.10$ spins/molecule. The lack of change in ϵ_{420} indicates that at both −295 and −326 mV only one $[Fe_4S_4]$ is reduced and that it is fully reduced. However, the $g_{z,y,x} = 2.04, 1.93, 1.89$ signal is typical of a magnetically isolated $S = 1/2$ $[Fe_4S_4]^{1+}$ system. Thus, the reduction must have occurred at another non-$[Fe_4S_4]$ site. The reduction must also have resulted in a diamagnetic non-$[Fe_4S_4]$ site to allow for an unperturbed $[Fe_4S_4]_C^{1+}$ ($S = 1/2$) signal. These data indicate that the [FeNi] site in wild-type CODH exhibits two redox couples. If an EPR unobservable ($S = 1$) Ni^{2+} species couples with $[Fe_4S_4]_C^{1+}$ ($S = 1/2$) to produce C_{red1}, then a one electron reduction would result in an EPR observable Ni^{1+} ($S = 1/2$) state that would also couple to $[Fe_4S_4]_C^{1+}$. This is not compatible with the observation that the reduction of a non-$[Fe_4S_4]$ species causes a decoupling of $[Fe_4S_4]_C^{1+}$. A two electron reduction of Ni^{2+} to $Ni^{2+}-H^-$ ($S = 0$) is possible, but would allow for neither the observation of the paramagnetic $g_{ave} = 2.16$ signal (albeit in small spin quantity) nor the existence of two redox couples with two EPR unobservable states (Ni^{3+} is also paramagnetic). Ragsdale and co-workers reported that for *Methanosarcina*

(17) Spangler, N. J.; Lindahl, P. A.; Bandarian, V.; Ludden, P. W. *J. Biol. Chem.* **1996**, *271*, 7973−7977.

thermophila CODH, a one-electron transition occurred at $E = -440$ mV producing g-values indicative of a magnetically isolated $[Fe_4S_4]_C^{1+}$ cubane. Another one-electron transition occurred at $E = -544$ mV. While the $E_m = -440$ mV transition was attributed to the reduction of $[Fe_4S_4]_B$ at the time, it is possible that the $E_m = -440$ mV transition represents the uncoupling of $[Fe_4S_4]_C^{1+}$ and the $E_m = -544$ mV transition is actually the reduction of $[Fe_4S_4]_B$.[18] Similarly, Hagen and co-workers reported the appearance of a single magnetically isolated $S = 1/2$ $[Fe_4S_4]^{1+}$ cluster at a potential of -322 mV in *Methanothrix soehngenii* CODH, whereas only C_{red1} was present at -280 mV. [19] These values are nearly identical with what we observe for the potentials of the non-$[Fe_4S_4]$ reduction proposed to uncouple $[Fe_4S_4]_C$ from the [FeNi] species. Based upon the data and these reports, we propose the most reasonable interpretation is that C_{red1} arises from the coupling of the $g_{ave} = 2.16$ $[(CO_L)Fe^{3+}\text{-}Ni^{2+}\text{-}H^-]^{4+}$ signal with the $g_{z,y,x} = 2.04$, 1.93, 1.89 $[Fe_4S_4]_C^{1+}$ signal. The Discussion section will address C_{red1} in greater detail.

(e) Evidence for Heterogeneity of the [FeNi] Signal of C_{red1} that can be Cured with CO Pretreatment (Evidence Supporting the Assignment of CO_L). Although the majority of the $g > 2.03$ region is arising from the $g_{ave} = 2.16$ signal, there are some features in the $g > 2.03$ region of the spectrum of CODH poised with naphthoquinone which are not seen in C531A CODH poised with indigo carmine. The presence of these signals indicates that the species producing the signal in the $g > 2.03$ region is not homogeneous. For instance, a feature at $g = 2.49$ (see Figure 3) is seen in wild-type CODH. This resonance occurs at a much higher g-value than any [FeNi] resonance observed in hydrogenases, and is not observed in indigo carmine-poised C531A CODH. Some of the resonances (e.g. the 2.32 feature versus the 2.30 and 2.25 features, see Figure 3) exhibit optimum intensities at slightly different temperatures (and powers, not shown). The possibility of heterogeneity is supported by our observation that CO pretreatment of CODH and subsequent removal of unbound CO by gel-filtration chromatography resulted in CODH with 30−40% increased initial CO-oxidation activity relative to CODH that was not CO pretreated. As we propose that the majority of the $g > 2.03$ features of wild-type CODH when poised with naphthoquinone are arising from the $[(CO_L)FeNi]$ cluster that produces the $g_{ave} = 2.16$ signal in C531A CODH, it is possible that the species giving rise to the $g > 2.03$ features undergoes the same handling-dependent, inactivating dissociation of bound CO_L observed with C531A CODH. We were interested in knowing whether any spectroscopic differences would be apparent in the $g > 2.03$ region between wild-type CODH either pretreated with CO or not, and subsequently poised with naphthoquinone. The results presented in the following sections indicate that differences do exist.

Figure 4 presents the wide range scan of the coupled $[(CO_L)\text{-}Fe^{3+}\text{-}Ni^{2+}\text{-}H^-]^{4+}\text{-}[Fe_4S_4]_C^{1+}$ system at 12 K, and Figure 5 focuses on the $[(CO_L)Fe^{3+}\text{-}Ni^{2+}\text{-}H^-]^{4+}$ (and other) resonances at 12 K, both with and without CO pretreatment before poising with naphthoquinone. It is clearly evident from Figure 4 that C_{red1} ($g_x = 1.71$) remains after CO pretreatment; however, Figure 5 shows that the $g > 2.03$ region of the spectrum is much simpler, suggesting a removal of [FeNi] cluster heterogeneity. Quantification of the spin-intensity of CO-pretreated naphthoquinone-poised CODH sample yielded a value of 0.20 ± 0.03 spins/molecule, identical within error to quinone-poised as-isolated CODH. Several pieces of information can be obtained from the appearance of the spectral features of 2-hydroxy-1,4-naphthoquinone-poised wild-type CODH with and without CO pretreatment. First, the increase in initial activity observed after CO pretreatment is probably involved with the decreased percentage of "unready" forms of the [FeNi] cluster, and not with a change in $[Fe_4S_4]_C$. We propose this because only the line shape of the region of the EPR spectrum containing the putative [FeNi] cluster resonances changes upon CO pretreatment. Second, the resonance at $g = 2.49$ disappears upon CO pretreatment, indicating it may be arising from an "unready" form of the [FeNi] cluster and probably is arising from a form of the [FeNi] cluster where a bound CO_L has dissociated. A possible origin of the 2.49 resonance is in a coupled form of a

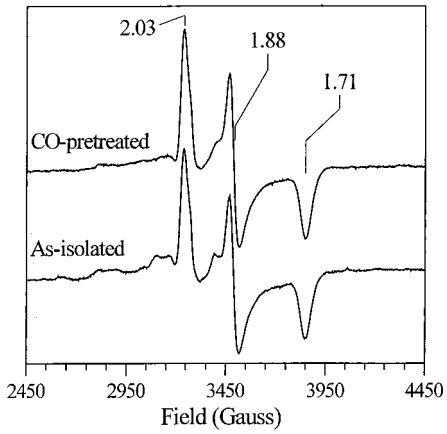

Figure 4. Effect of CO preincubation on the $g = 2$ region of the X-band EPR spectrum of *R. rubrum* CODH poised at -295 mV as in Figure 1. The two spectra were taken at 12 K (the temperature of maximum "C_{red1}" intensity) with and without CO preincubation. EPR conditions: microwave frequency = 9.23 GHz, microwave power = 1.0 mW, modulation amplitude = 10 G, modulation frequency = 100 kHz, time constant = 1 s.

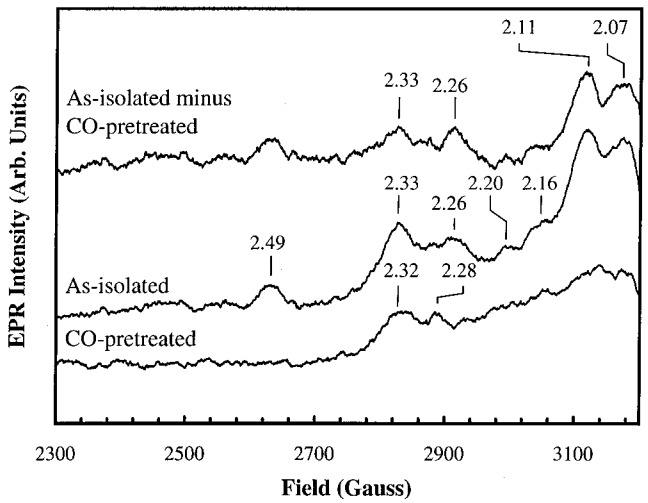

Figure 5. Effect of CO preincubation on the $g > 2.03$ region of the X-band EPR spectrum of *R. rubrum* CODH poised with dye as in Figure 1. Middle trace is the enzyme as-isolated, and then poised with dye as in Figure 1. Bottom trace is the enzyme as-isolated, then incubated with CO for 20 min before poising with dye after quickly removing excess CO by pumping and flushing 3×. The top trace is the difference spectrum of the middle trace minus the bottom trace. Temperature = 12 K. EPR conditions: microwave frequency = 9.23 GHz, microwave power = 1.0 mW, modulation amplitude = 10 G, modulation frequency = 100 kHz, time constant = 1 s.

(18) Lu, W.-P.; Jablonski, P. E.; Rasche, M.; Ferry, J. G.; Ragsdale, S. W. *J. Am. Chem. Soc.* **1994**, *116*, 9736−9742.

(19) Jetten, M. S.; Pierik, A. J.; Hagen, W. R. *Eur. J. Biochem.* **1991**, *202*, 1291−1297.

$[Fe^{2+}\text{-}Ni^{1+}]^{3+}$ or $[Fe^{2+}\text{-}Ni^{3+}\text{-}H^{-}]^{4+}$ cluster (these redox states are two of the proposed origins of so-called Ni−C signals in [NiFe] hydrogenases);[20] Ni−C has been shown to couple to the proximal $[Fe_4S_4]$ cluster in *D. gigas* hydrogenase.[21,22] It is also possible that it is arising from a $[Fe^{2+}Ni^{3+}]^{5+}$ species. Third, the [FeNi] cluster resonances that remain after CO pretreatment and that probably represent CO_L-bound forms of the [FeNi] cluster are quite broad and featureless, indicating coupling with the proximal $[Fe_4S_4]_C^{1+}$ cluster. This broadening can be somewhat alleviated at slightly higher temperatures (data not shown), but not to a great extent because the $[(CO_L)Fe^{3+}\text{-}Ni^{2+}\text{-}H^{-}]^{4+}$ and the $[Fe_4S_4]_C^{1+}$ cluster resonances have similar relaxation properties. Fourth, the deconvoluted spectrum, [(as-isolated) minus (CO-pretreated)], contains resonances which resemble a composite of several species observable in *C. vinosum* hydrogenase and *M. voltae* F_{420}-nonreducing hydrogenases under different conditions of CO treatment in the light and dark.[23]

Characterization of the Enzyme State Producing C_{red2A} (Characterization of Cobalt- and Zinc-Containing CODH). (a) Activities and Metal Content of Co- and Zn−CODH. Similar to previous reports, cobalt-CODH (Co-CODH) had a specific activity of 2.5 ± 0.6 units/mg, and could not be activated further by nickel addition in the presence of 0.2 mM methyl viologen and 0.2 mM dithionite.[13] Zn-CODH had no detectable activity, and was not activated by addition of nickel in the presence of methyl viologen (0.10 mM) and dithionite (0.20 mM). The previously reported iron contents of Ni-deficient, Ni-, Zn-, and Co-CODH were identical at 8.5 iron atoms/molecule of CODH.[12] Consistent with our other metal analysis results using the protein assay methods described in the Experimental Procedures section, we find 8.9 ± 0.3 Fe atoms/monomer. The amount of nickel was below the detection levels of the ICP-MS instrument (<0.04 ppm).

(b) EPR Spectroscopic Studies of Heterometal-Inserted Ni-Deficient CODH. The spectroscopic characteristics of Zn-CODH and Co-CODH were compared to those of Ni-CODH to determine if similar signals were present in the different forms. Figure 6A shows the X-band EPR spectrum of Ni-deficient CODH at the temperatures indicated, and Figure 6B shows a narrow range spectrum at high resolution of the region typically containing the resonance attributed to C_{red2} ($g_x = 1.75$). Two $[Fe_4S_4]^{1+}$ clusters can be deconvoluted by their differing relaxation properties as a function of temperature (Figure 6A).[24] The faster-relaxing cluster observable only below 30 K is typical of all-cysteinyl liganded clusters and is assigned to $[Fe_4S_4]_B^{1+}$. The exact g-values of $[Fe_4S_4]_B$ are difficult to determine due to the coupling described below. The slower-relaxing cluster ($g_{z,y,x}$ = 2.04, 1.93, 1.89) that is observable to 50 K and is well resolved at 35 K is atypical of $[Fe_4S_4]$ clusters with all-cysteinyl ligation and is attributed to $[Fe_4S_4]_C^{1+}$. At 35 K, nearly all of the observable EPR resonances arise from $[Fe_4S_4]_C^{1+}$. In agreement with previous reports,[11,13] there is a complete absence of the $g = 1.75$ feature of C_{red2} in Ni-deficient CODH (Figure 6B). However, the EPR spectrum at 4.7 K does not appear to be the simple sum of two isolated, noninteracting, $[Fe_4S_4]^{1+}$ clusters. A small upfield wing is present near $g = 2.09$, and the region between the inflection at $g = 1.93$ and the end of the apparent absorbance near $g = 1.85$ is somewhat distorted. These two features are maximized in fully reduced Ni-CODH (Figure 6G) at 4.7 K. However, in fully reduced (with excess dithionite) Ni-CODH, while the overall line shape of the $g = 2$ region remains similar, a $g = 1.755$ feature is also clearly visible (Figure 6H).

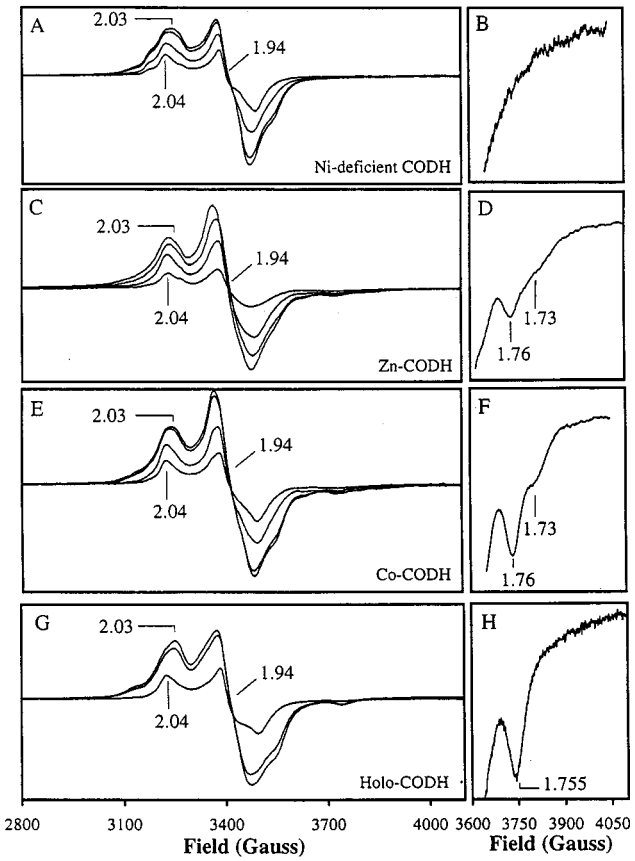

Figure 6. Comparison of the $g = 2$ region of the X-band EPR spectra of dithionite-treated *R. rubrum* CODH forms. (A) Ni-deficient CODH (80 μM) treated with 1 mM sodium dithionite and allowed to equilibrate for 5 min. Temperatures = 4.7, 10, 20,and 35 K. (B) 4-scan average of the $g \cong 1.75$ region of part A at 4.7 K. (C) Zn-constituted Ni-deficient CODH (100 μM) treated with sodium dithionite as in part A. Temperatures are the same as in part A. (D) 4-scan average of the $g \cong 1.75$ region of part B at 4.7 K.(E) Co-constituted Ni-deficient CODH (80 μM) treated with sodium dithionite as ipart A. Temperatures = 10, 20, and 40 K. (F) 4-scan average of the $g \cong 1.75$ region of part E at 4.7 K. (G) Ni-CODH treated with sodium dithionite as in part A. Temperatures = 4.7, 10, and 35 K.(H) 4-scan average of the $g \cong 1.75$ region of part G at 4.7 K. EPR conditions: microwave frequency = 9.23, microwave power = 1.0 mW, modulation amplitude = 10 G, modulation frequency = 100 kHz, time constant = 1 s.

The upfield wing is reminiscent of what is observed in the EPR spectrum of dithionite-reduced *Clostridium pasteurianum* 8Fe ferredoxin, which contains two weakly coupled $[Fe_4S_4]^{1+}$ ($S = 1/2$) clusters with a center−center distance of 12 Å.[25] Therefore, it is plausible that the resonance at $g \sim 1.75$ is the result of slightly stronger coupling between $[Fe_4S_4]_C^{1+}$ ($S = 1/2$) and $[Fe_4S_4]_B^{1+}$ ($S = 1/2$) which is induced only in the presence of a heterometal (normally Ni) in the active site. We hypothesized that the local conformation of the active site might

(20) Schneider, K.; Erkens, A.; Müller, A. *Naturwissenschaften* **1996**, *83*, 78−81.

(21) Dole, F.; Medina, M.; More, C.; Cammack, R.; Bertrand, P.; Guigliarelli, B. *Biochemistry* **1996**, *35*, 16399−16406.

(22) Guigliarelli, B.; More, C.; Fournel, A.; Asso, M.; Hatchikian, E. C.; Williams, R.; Cammack, R.; Bertrand, P. *Biochemistry* **1995**, *34*, 4781−4790.

(23) Duin, E. C. Exploring the Active Site of Nickel−Hydrogenases, Ph.D. Thesis, Universiteit van Amsterdam and Free University of Amsterdam: Amsterdam, 1996.

(24) Bonam, D.; Ludden, P. W. *J. Biol. Chem.* **1987**, *262*, 2980−2987.

(25) Cammack, R.; Patil, D. S.; Fernandez, V. M. *Biochem. Soc. Trans.* **1985**, *13*, 572−578.

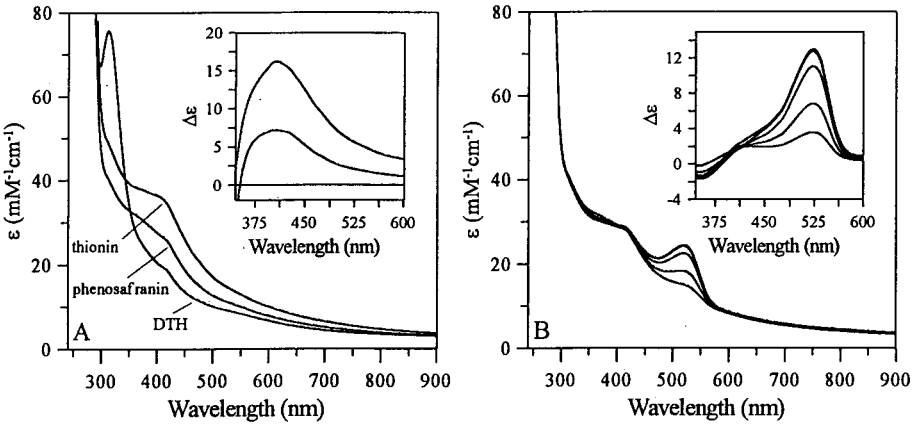

Figure 7. (A) UV−visible absorption spectra of *R. rubrum* CODH. Spectra were obtained for the enzyme in thionin-oxidized state, dithionite-treated state, and poised with 99% reduced phenosafranin (−326 mV). The enzyme concentration was 14 μM, while the concentration of 99% reduced phenosafranin was 500 μM. Inset: UV−visible absorption spectra of thionin-oxidized and 99% reduced phenosafranin-poised CODH minus dithionite-treated CODH. (B) UV−visible absorption spectra of *R. rubrum* CODH poised with 99% reduced phenosafranin and subsequently titrated with a 2 M $NaHCO_3$ solution to final $NaHCO_3$ concentrations of 1, 2, 3, 4, and 5 mM, and allowed to equilibrate for 10 min each. The starting solution was identical with that shown in part A as the phenosafranin trace. Inset: Subtraction of UV−visible absorption spectra of the $NaHCO_3$ titrations from the UV−visible absorption spectra of the starting enzyme solution poised with 99% reduced phenosafranin. For consistency, molar extinction coefficients are reported using enzyme concentration, rather than dye concentration.

be slightly different with and without heterometal present such that, in Ni-deficient CODH, the two clusters are never quite spatially close enough to produce the stronger coupling observed in fully reduced Ni-CODH. To assess this possibility, the redox-inert transition metal Zn^{2+} was incorporated into the vacant heterometal site of Ni-deficient CODH. Dithionite-treated samples of Zn-CODH show a resonance at $g = 1.76$, at a similar position to that observed in the fully reduced Ni-CODH ($g = 1.755$, compare Figure 6H and Figure 6D). However, this resonance is of weaker intensity and slightly different *g*-value than that seen in Ni-CODH. The spectrum of the entire region around $g = 2$ appears intermediate in line shape between Ni-deficient CODH and Ni-CODH, suggesting the $[Fe_4S_4]$ environment in Zn-CODH lies between those two "extremes". Co^{2+} was also incorporated into Ni-deficient CODH and the spectrum of this form of CODH is shown in Figure 6E. The overall spectrum of dithionite-treated Co-CODH appears to be intermediate in line shape between the spectra of dithionite-reduced Zn-CODH and Ni-CODH. The $g = 1.76$ feature is also observed with greater intensity in Co-incorporated CODH than in Zn-CODH (Figure 6F). The two $[Fe_4S_4]^{1+}$ clusters in Zn- and Co-incorporated CODH exhibit very similar relaxation properties to Ni-CODH and Ni-deficient CODH, as seen by temperature studies of the EPR spectrum. The $g = 1.76$ resonances have an observable maximum intensity at 4.7 K for both Zn-CODH and Co-CODH (not shown). As discussed in greater detail later, these results suggest that at least a portion of the $g = 1.755$ resonance observed in dithionite-reduced Ni-CODH may arise from the spin−spin coupling of $[Fe_4S_4]_C^{1+}$ ($S = 1/2$) with $[Fe_4S_4]_B^{1+}$ ($S = 1/2$).

An additional shoulder resonance at $g = 1.73$ is observed in both Zn-CODH and Co-CODH. As both of these forms of the enzyme have negligible activity and undetectable Ni levels, it is highly unlikely that the $g = 1.73$ shoulder arises from residual Ni-CODH. Additionally, the relaxation behavior of the $g = 1.73$ resonance parallels that of the $g = 1.76$ resonance, with maximum observable intensity at 4.7 K. Figure 2 showed that the maximum intensity of C_{red1} is at 12 K at 1.0 mW power (not 4 K). Therefore, the $g = 1.73$ shoulder may represent a population of enzyme in a slightly different conformation than that producing the 1.76 feature. It is also possible that the 1.76 and 1.73 features have their origin in the same coupling phenomenon and are both present whenever that particular coupling occurs. This shoulder is sometimes observed in Ni-CODH, but the exact conditions for its reproducible production have not been established. In contrast to Zn- and Co-CODH, the $g = 1.755$ feature in Ni-CODH has an intensity that varies from sample to sample. In addition, the $g = 1.755$ feature in dithionite-treated Ni-CODH samples varies from being equal in intensity at 4.5 and 10 K to being greatest in intensity at 10 K, and the position of the *g*-value varies within the range $g = 1.75$ to 1.76 (Figure 6H shows 1.755). Those samples that have a *g*-value closer to $g = 1.76$ have a lower temperature of maximum intensity, and are weaker in intensity in general (data not shown). We propose that this variability is a result of redox state heterogeneity of the [FeNi] cluster. Possible reasons for this redox state heterogeneity will be presented in the Discussion section.

Characterization of the Enzyme State Producing C_{red2B}. (a) UV−Visible Spectroscopy of CODH Poised at Different Potentials. Wild-type CODH was poised with 99% reduced phenosafranin at pH 7.5 (Figure 7). The UV−visible absorption spectrum shows that $\epsilon_{420} = 33.99\ mM^{-1}\ cm^{-1}$ for thionin-treated CODH, $\epsilon_{420} = 18.36\ mM^{-1}\ cm^{-1}$ for dithionite-treated CODH, and $\epsilon_{420} = 25.33\ mM^{-1}\ cm^{-1}$ for phenosafranin-poised CODH. Ninety-nine percent reduced phenosafranin ($E_m \cong -267$ mV versus SHE at pH 7.5; calculated $E = -326$ mV) was added to a final concentration of 0.5 mM, while the enzyme was of a final concentration of 0.014 mM. Ninety-nine percent reduced phenosafranin has negligible absorption in the region of 420 nm. Therefore, as the CODH concentration was very low, the donation of electrons to CODH resulted in a negligible increase in absorption in the dye. However, the molar extinction coefficient for CODH at 420 nm decreased by 46% upon treatment with dithionite, but only 26% upon treatment with phenosafranin (55% of that with dithionite). This indicates that only one of the $[Fe_4S_4]$ clusters of CODH was fully reduced upon addition of 99% reduced phenosafranin. Similarly, CODH poised with 95% reduced 2-hydroxy-1,4-naphthoquinone at pH 8.5 ($E_{calc} = -295$ mV) showed a decrease in the ϵ_{420} that was 50% of the decrease observed when treated with dithionite and nearly identical with what is observed with phenosafranin.

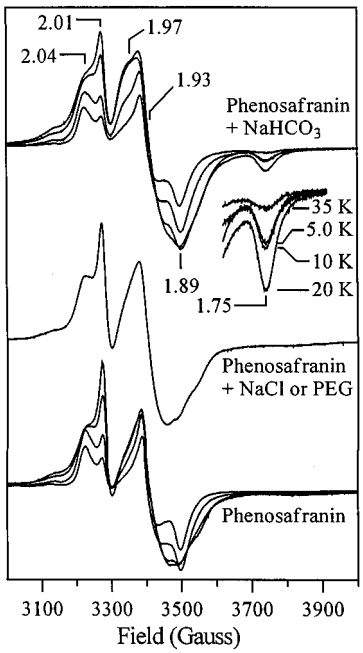

Figure 8. X-band EPR spectra of *R. rubrum* CODH poised with 99% reduced phenosafranin. CODH was diluted with buffer or PEG solution to a final concentration of 100 μM in all samples. CODH poised with 99% reduced phenosafranin contains 100 mM phenosafranin. Spectra were recorded at 5.0, 10, 20, and 35 K. Where added, PEG was to 50 vol % and NaCl was added to a final concentration of 400 mM. The EPR spectra of PEG-treated and NaCl-treated CODH are identical, and the spectrum presented was taken at 5.0 K. $NaHCO_3$ was added to a final concentration of 10 mM, and allowed to equilibrate for 10 min. Temperatures are 5.0, 10, 20, and 35 K. EPR conditions: microwave frequency = 9.23 GHz, microwave power = 1.0 mW, modulation amplitude = 10 G, modulation frequency = 100 kHz, time constant = 1 s.

Therefore, the redox states of the $[Fe_4S_4]$ clusters, which absorb in the 420 nm region, do not change significantly upon a change in potential from approximately −295 to −326 mV. However, the EPR spectra of CODH poised at these two potentials are dramatically different. Therefore, a non-$[Fe_4S_4]$ species must be reduced upon a shift from −295 to −326 mV. As described above, a paramagnetic [FeNi] cluster ($S = 1/2$) with a probable redox state of $[(CO_L)Fe^{3+}\text{-}Ni^{2+}\text{-}H^-]^{4+}$ is present in 2-hydroxy-1,4-naphthoquinone-poised CODH. We propose that the shift in redox potential from −295 to −326 mV causes a $[(CO_L)\text{-}Fe^{3+}\text{-}Ni^{2+}\text{-}H^-]^{4+}/[(CO_L)Fe^{2+}\text{-}Ni^{2+}\text{-}H^-]^{3+}$ transition. This assignment is consistent with the lack of an observed change in ϵ_{420} associated with the redox event.

(b) EPR Spectroscopy of CODH Poised with 99% Reduced Phenosafranin without and with $NaHCO_3$ (Preparation of the Enzyme State Producing C_{red2B}). The EPR spectra of phenosafranin-treated CODH at 5.0, 10, 20, and 35 K are shown in Figure 8. Only the same slow-relaxing cluster observed in dithionite-treated CODH (Ni- and Ni-deficient) and assigned to $[Fe_4S_4]_C^{1+}$ is observed. The lack of perturbation of the $[Fe_4S_4]_C^{1+}$ signals ($g_{z,y,x} = 2.04, 1.93, 1.89$) from those of typical $[Fe_4S_4]^{1+}$ clusters (i.e. C_{red1} is not observed) suggests that the majority of the [FeNi] cluster has been reduced to a diamagnetic oxidation state (proposed to be $[(CO_L)Fe^{2+}\text{-}Ni^{2+}\text{-}H^-]^{3+}$), resulting in a magnetically isolated $[Fe_4S_4]_C^{1+}$ cluster spin in the major fraction of enzyme sample. The spin intensity of the $g = 2$ region quantifies to 0.65 ± 0.05 spins/molecule. An additional resonance at $g = 2.01$ is also evident. The intensity of this resonance is maximal at 5.0 K, indicating that it is not due to a small spin-quantity of a radical species (e.g., phenosafranin radical). One plausible explanation is that it is a very small fraction of $[Fe_3S_4]_C^{1+}$ (a breakdown product of $[Fe_4S_4]_C$) similar to that observed in 2-hydroxy-1,4-naphthoquinone-treated CODH at 55 K (see Figure 2) (the same batch of enzyme was used in both analyses). The signal amplitude seems impressive due to the nearly isotropic nature of resonances arising from $[Fe_3S_4]^{1+}$ clusters. Consistent with this proposal is the absence of the signal in dithionite-treated samples, suggesting a reduction to the $[Fe_3S_4]_C^0$ ($S = 2$) redox state. Additionally, a very small amount of another fast-relaxing species is present which causes a distortion of the $g = 1.93-1.85$ region at low temperatures. This probably arises from a very small spin quantity of $[Fe_4S_4]_B^{1+}$ present at this potential. The amount of $[Fe_4S_4]_B^{1+}$ must be very small because the UV−visible absorption spectra indicate that only one $[Fe_4S_4]$ cluster is reduced upon treatment with phenosafranin and at 20 K the amplitude of the EPR spectrum of $[Fe_4S_4]_C^{1+}$ is nearly the same as at 5.0 K, unlike when $[Fe_4S_4]_B$ is reduced. The small upfield wing near $g = 2.09$ that is most prominent in samples at 5.0 K is proposed to arise from that small fraction of CODH that has $[Fe_4S_4]_B^{1+}$ present in addition to $[Fe_4S_4]_C^{1+}$. The wing is proposed to arise from the spin−spin coupling of $[Fe_4S_4]_C^{1+}$ with $[Fe_4S_4]_B^{1+}$ described in the previous section. An extremely small amount of the paramagnetic [FeNi] species described earlier is also present in the g > 2.10 region (data not shown), and will be further discussed below. Therefore, we propose that phenosafranin-treated CODH has the following paramagnetic species present in the $g = 2$ region, in decreasing order of relative abundance: $[Fe_4S_4]_C^{1+} >>> [FeNi]^{?+} \cong [Fe_4S_4]_B^{1+} > [Fe_3S_4]_C^{1+}$. However, we propose that the large majority of the CODH molecules have the following arrangement of clusters:

$$[Fe_4S_4]_C^{1+}\ (S = 1/2),\ [(CO_L)Fe^{2+}\text{-}Ni^{2+}\text{-}H^-]^{3+}\ (S = 0),\ \text{and}\ [Fe_4S_4]_B^{2+}\ (S = 0)$$

The same phenosafranin-poised sample described in the UV−visible absorption experiment described above (Figure 7A) was then sequentially titrated with a $NaHCO_3$ solution to final concentrations of 1, 2, 3, 4, and 5 mM $NaHCO_3$ (Figure 7B). This treatment resulted in the $[CO_2]$-dependent partial oxidation of the reduced phenosafranin (as indicated by an increase in absorbance at 530 nm), while the control without CODH added did not (not shown). The UV−visible absorption spectra of the CODH solution titrated with the described $NaHCO_3$ concentrations minus the starting point of the CODH solution poised with 99% reduced phenosafranin (Figure 7B, inset) is nearly identical with the spectrum of oxidized phenosafranin (not shown), indicating that the $[Fe_4S_4]$ cluster redox states do not change. In particular, the ϵ_{420} (which is due to absorbance by the $[Fe_4S_4]$ clusters) is almost completely unchanged. However, the EPR spectrum is dramatically altered in a 1 mM sample of CODH poised with 99% reduced phenosafranin and subsequently treated with 10 mM $NaHCO_3$ (Figure 8, top trace), with a new feature appearing at $g = 1.75$. A salt effect is not the cause of this change, as the EPR spectrum is unaltered by the addition to the bicarbonate-untreated CODH sample of solid NaCl to a final concentration of 400 mM (Figure 8, middle trace). Additionally, a crowding effect[26] was eliminated, as PEG to 50 vol % does not alter the EPR spectrum either (Figure 8, middle trace).

The $g = 1.75$ resonance was examined as a function of temperature. The $g = 1.76$ resonance discussed in the previous

(26) Fulton, A. B. *Cell* **1982**, *30*, 345−347.

section arises from coupling of $[Fe_4S_4]_B^{1+}$ and $[Fe_4S_4]_C^{1+}$, and thus follows the temperature dependence of $[Fe_4S_4]_B^{1+}$, being of maximum observable intensity at 4.7 K at 1 mW microwave power. The $g = 1.75$ resonance discussed in this section, however, has a maximum intensity at 20 K and is greatly saturated at 4.7 K (also at 1 mW power). The relaxation properties and the method of generation of the two species indicate that the $g = 1.75$ resonance does not arise from the spin-coupling of the same two species that produce the $g = 1.76$ resonance in Zn- and Co-CODH.

Discussion

The primary proposals made based upon spectroscopic studies of *R. rubrum* CODH are as follows: C_{red1} is the result of the spin−spin coupling of two $S = 1/2$ signals proposed to be arising from $[(CO_L)Fe^{3+}\text{-}Ni^{2+}\text{-}H^-]^{4+}$ and $[Fe_4S_4]_C^{1+}$ cluster redox states; spectroscopic features at $g = 1.75-1.76$, previously attributed to a state of CODH referred to as C_{red2}, arise from two distinct redox states of the enzyme.; C_{red2A} is the result of the spin−spin coupling of two $S = 1/2$ signals proposed to be arising from $[Fe_4S_4]_C^{1+}$ and $[Fe_4S_4]_B^{1+}$ cluster redox states; and C_{red2B} is the result of the spin−spin coupling of an $S = 1$ and an $S = 1/2$ signal proposed to be arising from $[(CO_L)Fe^{2+}\text{-}Ni^{2+}]^{4+}$ and $[Fe_4S_4]_C^{1+}$ cluster redox states, respectively.

C_{red1}. The Results section presented arguments that C_{red1} arises from the coupling of $[(CO_L)Fe^{3+}\text{-}Ni^{2+}\text{-}H^-]^{4+}$ ($S = 1/2$, $g_{ave} = 2.16$) with $[Fe_4S_4]_C^{1+}$ ($S = 1/2$, $g_{z,y,x} = 2.04, 1.93, 1.89$). Naphthoquinone-poised CODH was shown to exhibit perturbed signals from both of these species, but in low overall spin quantity. As discussed in Part 1, we believe *R. rubrum* CODH to be comprised of 9 Fe atoms arranged as follows: $[Fe_4S_4]_B$, $[Fe_4S_4]_C$, and [FeNi]. Hu et al. reported that in *R. rubrum* CODH poised at −300 mV, 70% of all iron has diamagnetic character.[1] At this potential, the B cluster is $[Fe_4S_4]^{2+}$, $S = 0$, and thus accounts for 44% of the total iron content. This leaves $(70 - 44) = 26\%$ of the total Fe content arising from C-site clusters (the $[Fe_4S_4]_C$ and [FeNi] sites) with diamagnetic character. The remaining 30% of the total Fe arises from C-site clusters with paramagnetic character, of which a significant portion of $[Fe_4S_4]_C$ is in an $S = 3/2$ ground state (when magnetically isolated, as observable in the fully reduced enzyme). From our experience with multiple samples, the line shape of the EPR signal reported by Hu et al. indicates the presence of a small amount of magnetically isolated ($S = 1/2$) $[Fe_4S_4]_C^{1+}$ (indicating some of the iron from the putative [FeNi] cluster is diamagnetic). The low spin quantity of the $g = 2$ region of C_{red1} was proposed to be due to a combination of the diamagnetic component and an $S = 3/2$ state of the C site clusters.

Despite the proposed reasons for the low spin intensity of the C_{red1} features, the UV−visible data in our present study indicate that at −300 mV all $[Fe_4S_4]_C$ is in the $[Fe_4S_4]^{1+}$ state (whether $S = 3/2$ or 1/2), so that ∼56% of the total Fe content should be paramagnetic, rather than the 30% determined by Mössbauer. The EPR spectrum of the Mössbauer sample reported by Hu et al. was nearly identical with that shown in Figure 4C of Spangler et al.[17] We propose the EPR spectrum of Figure 4C was comprised of largely C_{red1} signals, but also a small fraction of magnetically isolated $[Fe_4S_4]_C^{1+}$. As Figure 4 of Spangler et al. showed,[17] the CODH sample exhibiting this particular EPR spectrum had a 47% decrease in ϵ_{420} from the thionin-oxidized state versus the decrease in ϵ_{420} when the enzyme was treated with excess dithionite. This value of 47% is consistent with our present data (this work) that show CODH exhibits a 50% decrease in ϵ_{420} at both −295 and −326 mV (versus the decrease when the enzyme is treated with dithionite). A 47% reduction of ϵ_{420} should yield more paramagnetic $[Fe_4S_4]$ clusters than were detected by Mössbauer. We propose this discrepancy can be resolved as follows: Because a small amount of the $g_{ave} = 2.16$ signal can be observed at −295 mV, we have attempted to simulate[33] the C_{red1} state as the result of simple dipolar coupling between the $g_{ave} = 2.16$ signal and the $[Fe_4S_4]_C$ cluster with $g_{z,y,x} = 2.04, 1.93, 1.88$ (data not shown). Preliminary results indicated that a very strong coupling was needed to achieve g-values similar to the C_{red1} signals (2.03, 1.88, 1.71). The dipolar coupling needed to produce the observed g-values for C_{red1} was greater than that for which a simple dipolar model is reasonable: $D = 0.15\ cm^{-1}$, which requires a distance between the two spins of less than 3 Å. To have a meaningful physical model, it would be necessary to introduce significant exchange coupling into the EPR simulation. If this is the case, then a possible explanation for the diamagnetic component is immediately presented, namely a strong enough antiferromagnetic exchange between the two $S = 1/2$ sites (the [FeNi] site with $g_{ave} = 2.16$ and $[Fe_4S_4]_C^{1+}$ with an $S = 1/2$ component with $g_{z,y,x} = 2.04, 1.93, 1.89$) may yield a resultant $S_{tot} = |1/2 - 1/2| = 0$ ground state. No well-defined $S = 3/2$ component of [Fe4S4]C is observed in significant quantity in CODH poised at −300 mV, yet is present in the reduced state of the enzyme. This suggests an interaction between the $S = 3/2$ component of $[Fe_4S_4]_C$ with the $S = 1/2$ $g_{ave} = 2.16$ signal. It is unclear what the spectroscopic result would be of an exchange coupling between these two sites. For antiferromagnetic coupling, $S_{tot} = |3/2 - 1/2| = 1$, which would likely be EPR-unobservable. However, weaker exchange coupling of the $S = 3/2$ component with the $g_{ave} = 2.16$ signal might produce anomalous resonances in the $g = 4-6$ region of the EPR spectrum, such as are often observed for the enzyme state producing C_{red1}.

The exact coupling scheme producing the EPR-observable $g \sim 2$ fraction of cluster states at −295 mV is not certain. It is possible that several discrete interactions ranging from dipolar coupling to strong exchange coupling occur in CODH. A population exhibiting mainly dipolar coupling interaction with weaker exchange coupling interaction may account for the observation in low spin intensity of the broadened $g_{ave} = 2.16$ signal and the $g_{z,y,x} = 2.03.\ 1.88, 1.71$ signal. Several reports have indicated that the production of C_{red1} from C_{ox} is a one-electron process. However, these reports only followed the intensity of the apparent g_z or g_x features of the 2.03, 1.88, 1.71 signal versus baseline, or the peak-to-trough intensity of the apparent g_y feature. The forementioned earlier work in our laboratory[17] followed only the change in ϵ_{420} of the UV−visible absorption spectrum, which is derived entirely from the $[Fe_4S_4]$ clusters (and not the proposed [FeNi] cluster). It is possible that the 2.03, 1.88, 1.71 features arise only from the $[Fe_4S_4]$ half of the coupled system. We are planning redox titrations of the entire $g = 2$ region (including the $g > 2.03$ resonances) to directly test the hypothesis that the C_{ox}/C_{red1} transition is actually a two-electron process. Nevertheless, a fit to a one-electron process would suggest against the possibility that the $g = 2.03, 1.88, 1.71$ features arise from an $S = 1$ state (e.g. $S_{tot} = |3/2 - 1/2| = 1$; as described above), the production of which would require two electrons.

Upon a decrease in potential from −295 to −326 mV, we propose one species of this exchange coupled dimeric system (i.e. the [FeNi] cluster) is reduced. The reduced species is proposed to be $S = 0$. The reduction of one species of the exchange coupled dimeric system to a diamagnetic state is

proposed to result in the observation of a magnetically isolated $S = 1/2$ form of the other species (namely $[Fe_4S_4]_C$). Such a reduction can reasonably explain the increase in spin quantitation from 0.20 to 0.65 spins/mol without a concurrent decrease in ϵ_{420} observed when the potential is reduced. Dithionite-reduced Ni-deficient CODH (1.58 ± 0.10), Zn-CODH (1.40 ± 0.10), and Co-CODH (1.27 ± 0.10) (WT forms) all exhibit ~1.50 spins/mol in the $g \sim 2$ region (preparation dependent). Assuming that ~1 spin/monomer arises from $[Fe_4S_4]_B^{1+}$, the value ~0.50 ± 0.10 spins/mol thus accounts for the $S = 1/2$ component of $[Fe_4S_4]_C^{1+}$ at both −530 (dithionite-reduced) and −326 mV (phenosafranin-treated).

Finally, in our simulations, we did not test the possibility that in certain states (e.g. the C_{red1} state), perhaps as a result of conformational changes, the *intrinsic g*-values of $[Fe_4S_4]_C$ might be shifted from those in the magnetically isolated state (i.e. away from 2.04, 1.93, 1.89). Recent work with *Pyrococcus furiosus* ferredoxin has shown that the position of the liganding serinate in $[Fe_4S_4](Cys)_3(Ser)$ clusters (i.e. at the Fe1, Fe2, Fe3, or Fe4 position) significantly affects the *g*-values of the $[Fe_4S_4]^{1+}$ cluster, suggesting that subtle changes in electron distribution within the cube lead to large changes in the observed *g*-values.[27] Given the possibility that the *g*-values of $[Fe_4S_4]_C^{1+}$ could be altered by a change in local environment, the parameter set would become too large for meaningful simulations.

Our analysis of *R. rubrum* CODH poised in the state producing the C_{red1} reveals that the assigned [FeNi] signals are heterogeneous in as-isolated CODH (i.e. not CO-pretreated). The observed heterogeneity is consistent with heterogeneity reported for the Ni environment in the C-cluster of *C. thermoaceticum* CODH.[28] This heterogeneity in *C. thermoaceticum* was at the time not understood; however, it can be explained by the data shown in Figures 4 and 5. In *R. rubrum* CODH, the fraction of $[FeNi]^{n+}$ that is proposed to be catalytically "unready" and that is "cured" by CO-pretreatment (see Figure 5) is presumably of a different reduction potential than the proposed catalytically "ready" $[(CO_L)Fe^{3+}\text{-}Ni^{2+}\text{-}H^-]^{4+}$ forms, and may have a different electron distribution within the [FeNi] cluster. While we are in the process of addressing this issue with dye-mediated EPR-monitored redox titrations, it is probable that the $[(CO_L)Fe^{3+}\text{-}Ni^{2+}\text{-}H^-]^{4+}$ resonance in C531A CODH reequilibrates with buffer according to the following equation:

$$[(CO_L)Fe^{3+}\text{-}Ni^{2+}\text{-}H^-]^{4+} \rightleftarrows [FeNi\text{-}H^-]^{n+} + CO_{buffer}$$

The system to the right in the above equation is not paramagnetic when poised with indigo carmine in C531A, suggesting a lower reduction potential for the cluster (see Part 1) based upon the electron-withdrawing nature of CO.

Taken together, the results presented here support the interpretation that a nonsubstrate but activating CO (referred to as CO_L) binds to the [FeNi] cluster in wild-type CODH, similar to the binding proposed for C531A CODH. However, as Figures 3−5 show, when reduced the catalytically "unready" forms of the [FeNi] cluster also couple to $[Fe_4S_4]_C^{1+}$. The presence of sample-dependent amounts of "unready" forms of [FeNi] cluster may help to explain the variability in the broadening of C_{red1} by ^{61}Ni. This broadening has ranged from less than 2 G[1] to 9 G.[10] The "unready" forms (CO_L-dissociated) of the [FeNi] cluster, when reduced, might produce a $[Fe^{2+}\text{-}Ni^{1+}]^{3+}$ or $[Fe^{2+}\text{-}Ni^{3+}\text{-}H^-]^{4+}$ ($S = 1/2$) cluster, rather than a $[(CO_L)Fe^{3+}\text{-}Ni^{2+}\text{-}H^-]^{4+}$ ($S = 1/2$, $g_{ave} = 2.16$) cluster. Based upon Figures 3 and 5, the following hypothesis is offered. These possible $[Fe^{2+}\text{-}Ni^{1+}]^{3+}$ or $[Fe^{2+}\text{-}Ni^{3+}\text{-}H^-]^{4+}$ forms of the [FeNi] cluster also couple with $[Fe_4S_4]_C^{1+}$ to yield a similar line shape for the coupled $[Fe_4S_4]_C^{1+}$ component of C_{red1}. However, it is only these "unready" forms of the [FeNi] cluster (which lack CO_L and have unpaired spin-density on the Ni atom) that produce ^{61}Ni broadening. Therefore, sample-dependent amounts of "unready" [FeNi] cluster result in sample-dependent ^{61}Ni broadening values. The determination of the exact nature and reduction potentials of both the catalytically "ready" and "unready" (but activatable) forms of the [FeNi] cluster will be a focus of future research.

C_{red2A}. EPR spectroscopic studies of Zn- and Co-CODH have revealed that the spin−spin coupling of $[Fe_4S_4]_C^{1+}$ ($S = 1/2$) with $[Fe_4S_4]_B^{1+}$ ($S = 1/2$) produces a resonance at $g = 1.76$ that we term C_{red2A}. We find that a spectroscopic feature resembling the C_{red2} ($g = 1.755$) seen in dithionite-treated *R. rubrum* Ni-CODH is observed with maximal intensity in Zn-CODH and Co-CODH when both $[Fe_4S_4]$ clusters are reduced, but is positioned at $g = 1.76$. The maximal observed intensity of C_{red2A} in Zn- and Co-CODH does not parallel that of C_{red1} ($g_x = 1.71$), which has a maximum intensity at 12 K, as shown in Figure 2. It also does not parallel that of C_{red2B} (Figure 8, top trace), which has a maximum intensity at 20 K (see Figure 8, expansion of top trace). It does, however, parallel the intensity of the fast-relaxing $[Fe_4S_4]_B^{1+}$ cluster that has maximal observed intensity at 4.7 K. This signal was perplexing, because it at first seemed to be the same as C_{red2B} (it is in a similar position). It is only because of the unique ability of *R. rubrum* CODH to be isolated in a Ni-deficient form that this signal could be understood. Replacing the Ni of the [FeNi] cluster with Zn should result in a diamagnetic ($S = 0$) and EPR unobservable [FeZn] cluster if the iron remains in a low spin ferrous configuration. We propose that the iron atom does remain in the low spin ferrous configuration in the majority of Zn-CODH, as we observe no other signals in the EPR spectrum of dithionite-treated Zn-CODH in the low field region that would indicate a $S = 2$ species from a high-spin ferrous Fe (data not shown). A [FeZn] ($S = 0$) cluster will not affect the EPR properties of $[Fe_4S_4]_C$ or $[Fe_4S_4]_B$. Therefore, because the C_{red2A} feature is observed in dithionite-treated Zn-CODH without the presence of a paramagnetic center other than $[Fe_4S_4]_B^{1+}$ and $[Fe_4S_4]_C^{1+}$, C_{red2A} has its origin in the coupling of the two $[Fe_4S_4]^{1+}$ cluster spins. Consistent with this assignment is the appearance in reduced Zn-CODH, Co-CODH, and Ni-CODH of an upfield wing ($g \sim 2.09$) and distortions of the region between the inflection at $g = 1.93$ and the end of the apparent absorbance near $g = 1.85$. These characteristics are similar to those observed in *C. pasteurianum* 8Fe ferredoxin,[25] where two $[Fe_4S_4]^{1+}$ ($S = 1/2$) clusters also couple. It seems likely that when both $[Fe_4S_4]_C$ and $[Fe_4S_4]_B$ are reduced in Ni-CODH, C_{red2A} will also be present.

Because dithionite-treated Zn-CODH and Co-CODH exhibit EPR spectra which are nearly identical (see Figure 6), Co-CODH must contain a [FeCo] cluster which is diamagnetic so that the coupling scheme producing C_{red2A} is consistent between the two forms. With a [FeCo] cluster it cannot be assumed that the Fe atom remains low spin ferrous ($S = 0$) but, depending upon the conditions and redox state, may be present as a low spin ferric ($S = 1/2$) atom as it is in the [FeNi] cluster state producing the $g_{ave} = 2.16$ signal. In Co-CODH, if the iron atom is low spin ferrous, the cobalt atom must necessarily be diamagnetic. However, if the iron atom is low spin ferric, the

(27) Brereton, P. S.; Duderstadt, R. E.; Staples, C. R.; Johnson, M. K.; Adams, M. W. W. *Biochemistry* **1999**, *38*, 10594−10605.

(28) Shin, W.; Anderson, M. E.; Lindahl, P. A. *J. Am. Chem. Soc.* **1993**, *115*, 5522−5526.

cobalt atom should have one unpaired electron such that antiferromagnetic coupling of the two $S = 1/2$ spins can result in a diamagnetic [FeCo] cluster. Therefore, if the iron atom is low spin ferrous, the cobalt atom must necessarily be low spin Co^{3+} ($S = 0$), and if the iron atom is low spin ferric, the cobalt atom must necessarily be low spin Co^{2+} ($S = 1/2$). These two conditions need not be exclusionary (i.e., an equilibrium might exist). The above requirements may have implications for the coordination geometry of the Co atom within Co-CODH, and in turn may imply a coordination geometry for Ni within Ni-CODH. These implications will be more thoroughly discussed in a future publication that will include other redox states of Co-CODH.

The interpretation of the $g = 1.755$ feature in dithionite-treated Ni-CODH is more difficult than it is for Zn-CODH. In a previous report,[1] the spectroscopic feature referred to as "C_{red2}" in dithionite-treated Ni-CODH could only be simulated as the g_x value ($g = 1.75$) of a species with $g_z = 1.97$ and $g_y = 1.87$. However, the g_z and g_y resonances were never directly observed, a problem that was attributed to the interference of $[Fe_4S_4]_B^{1+}$ in the same region of the spectrum. As described in the Results section, the $g = 1.755$ resonance in dithionite-treated Ni-CODH does not have exactly the same relaxation properties (or *g*-value) as it does in Zn- and Co-CODH. It also has variability in position and intensity. We propose that dithionite-reduced Ni-CODH has a mixture of coupling schemes which both give rise to a feature near $g = 1.75$. As described above, the first coupling scheme produces C_{red2A}. The second produces C_{red2B}. In Ni-CODH the redox state of the proposed [FeNi] cluster has dramatic effects upon the EPR spectrum. C_{red2B} ($g_x = 1.75$), which is proposed to arise from the coupling of $[(CO_L)Fe^{2+}\text{-}Ni^{2+}]^{4+}$ ($S = 1$) with $[Fe_4S_4]_C^{1+}$ ($S = 1/2$), has a maximum intensity at 20 K and is more intense than the $g = 1.76$ resonance. When the [FeNi] cluster is in the presumed $[(CO_L)Fe^{2+}\text{-}Ni^{2+}]^{4+}$ redox state (fully oxidized, $S = 1$), but both $[Fe_4S_4]$ clusters are reduced, the $g \sim 1.75$ region should be a composite of the $[Fe_4S_4]_B^{1+}/[Fe_4S_4]_C^{1+}$ coupling (C_{red2A}, $g = 1.76$) and the $[(CO_L)Fe^{2+}\text{-}Ni^{2+}]^{4+}/[Fe_4S_4]_C^{1+}$ coupling (C_{red2B}, $g = 1.75$). We propose that in Ni-CODH a mixture of $[(CO_L)Fe^{2+}\text{-}Ni^{2+}\text{-}H^-]^{3+}$ ($S = 0$) and $[Fe^{2+}\text{-}Ni^{2+}]^{4+}$ ($S = 1$) always exists when the enzyme is treated with CO, even when CO is in very large excess. The CO/CO_2 equilibrium has been reported previously,[9] and is described in relation to an $[(CO_L)Fe^{2+}\text{-}Ni^{2+}]^{4+}/[(CO_L)Fe^{2+}\text{-}Ni^{2+}\text{-}H^-]^{3+}$ equilibrium in the next section. The combination of C_{red2B} (with a maximum intensity at 20 K, a greater intensity in general, and in variable amounts) with C_{red2A} (with a maximum observed intensity at 4.7 K, and a lesser intensity in general) produces the variability in the maximum intensity, exact *g*-value, and relaxation properties as a function of temperature of the $g = 1.75-1.76$ feature in Ni-CODH when treated with a large excess of CO. This same combination causes variability when CODH is treated with dithionite because dithionite often contains 15% sodium bicarbonate (a source of CO_2). To minimize the possibility of a CO_2/CO equilibrium, ultrapure sodium dithionite was used for our experiments. However, even with this ultrapure dithionite, the $g = 1.755$ feature still does not have identical relaxation properties, line shape, and *g*-values in Ni-CODH when compared to the $g = 1.76$ feature of Zn- or Co-CODH. It is possible that a similar equilibrium of oxidized and reduced species may occur with dithionite breakdown products such that 100% reduction of $[(CO_L)Fe^{2+}\text{-}Ni^{2+}]^{4+}$ to $[(CO_L)Fe^{2+}\text{-}Ni^{2+}\text{-}H^-]^{3+}$ may not be possible, but the equilibrium does lie far to the side of $[(CO_L)Fe^{2+}\text{-}Ni^{2+}\text{-}H^-]^{3+}$.

C_{red2B}. The spin−spin coupling of $[Fe_4S_4]_C^{1+}$ ($S = 1/2$) with $[(CO_L)Fe^{2+}\text{-}Ni^{2+}]^{4+}$ ($S = 1$) is proposed to produce C_{red2B}. Poising of *R. rubrum* CODH with 99% reduced phenosafranin at pH 7.5 ($E_m \cong -267$ mV versus SHE at pH 7.5; calculated $E = -326$ mV) results in the disappearance of the C_{red1} coupling resonances. $[Fe_4S_4]_C^{1+}$ ($S = 1/2$) is thus not spin-coupled to a paramagnetic [FeNi] cluster as we propose it is in 95%-reduced 2-hydroxy-1,4 -naphthoquinone-poised ($E_m \cong -257$ mV versus SHE at pH 8.5; calculated $E = -295$ mV) CODH. At −326 mV $[Fe_4S_4]_C^{1+}$ is still present as a slow-relaxing species observable to greater than 35 K (Figure 8). This indicates that the [FeNi] cluster has been reduced, presumably to the $[(CO_L)\text{-}Fe^{2+}\text{-}Ni^{2+}\text{-}H^-]^{3+}$ ($S = 0$) oxidation state. For the most part, the system can be described as $[Fe_4S_4]_C^{1+}$, $[(CO_L)Fe^{2+}\text{-}Ni^{2+}\text{-}H^-]^{3+}$, and $[Fe_4S_4]_B2+$. With this as the starting point, CO_2 in the form of $NaHCO_3$ was added to the system. It is known that the reaction of CO to CO_2 follows the equation:

$$CO + H_2O \rightleftarrows CO_2 + 2e^- + 2H^+$$

As this is a reversible process, it is quite reasonable that the system can be forced to the left by addition of a large excess of product when the enzyme is in the appropriate starting redox states. We propose that this is exactly what has been accomplished by poising the system with 99% reduced phenosafranin and adding CO_2 in the form of sodium bicarbonate. The [FeNi] cluster, initially in the $[(CO_L)Fe^{2+}\text{-}Ni^{2+}\text{-}H^-]^{3+}$ ($S = 0$) oxidation state, reduces CO_2 to CO, with the concurrent production of water and oxidation of the [FeNi] cluster to the $[(CO_L)Fe^{2+}\text{-}Ni^{2+}]^{4+}$ ($S = 1$) oxidation state. Turnover is accomplished by direct re-reduction of [FeNi] cluster with reduced phenosafranin (a 2 e^- donor), which is in large excess, resulting in the accumulation of oxidized phenosafranin in the UV−visible absorption spectrum. Production of CO from the above system has been confirmed by monitoring changes in the position and intensity of the Soret band of hemoglobin which are characteristic of CO binding (data not shown).[14] It is important to note that the redox states of $[Fe_4S_4]_B$ and $[Fe_4S_4]_C$ did not change during this experiment, thus the [FeNi] cluster alone is able to catalyze the two-electron reduction of CO_2.

There are only a limited number of redox states from which C_{red2B} could arise. An EPR observable [FeNi] species can be ruled out based upon the position of the *g*-value ($g =$ much less than 2, whereas typical paramagnetic Ni and low spin ferric iron signals are positioned at $g > 2$), and the fact that we have already observed the paramagnetic ($S = 1/2$) [FeNi] cluster as described in Part 1 of this series. $[Fe_4S_4]_C^{1+}$ coupled to $[Fe_4S_4]_B^{1+}$ (C_{red2A}, see previous discussion section) can likewise be ruled out because of the differing temperature of maximum intensity and method of generation. Coupling involving $[Fe_4S_4]_B^{1+}$ with any form of the [FeNi] cluster can probably be ruled out based upon the differing relaxation properties of this C_{red2B} and $[Fe_4S_4]_B^{1+}$ and the fact that the UV−visible absorption spectrum indicates that only one $[Fe_4S_4]$ is reduced. $[FeNi]^{n+}$ ($S = 1/2$) coupled to $[Fe_4S_4]_C^{1+}$ is more difficult to eliminate, because we do observe a very small amount of a $[FeNi]^{n+}$ ($S = 1/2$) species still present in the phenosafranin-treated CODH. Therefore, it is possible that CO_2 addition in the presence of reduced phenosafranin produces a form of C_{red1}-like coupling with slightly different properties, perhaps involving a conformational change. However, because two electrons are required for CO_2 reduction to CO, and a two-electron donating dye is used (and oxidized), this does not seem likely. Additionally, the minority $[FeNi]^{n+}$ species observed in CODH poised with 99% reduced phenosafranin (not shown) are identical to the $[FeNi]^{n+}$ species

which were identified as probable "unready" forms in our studies of C_{red1}. That is to say, CO preincubated CODH (which was subsequently oxidized by thionin and had thionin removed by chromatography) poised with 99% reduced 2-hydroxy-1,4-naphthoquinone *minus* as-isolated (not preincubated with CO) CODH under the same conditions results in a spectrum in the $g > 2.03$ region that is nearly identical with the $[FeNi]^{3+}$ species observed in 99% reduced phenosafranin-treated CODH (with the exception of the 2.49 species). CO preincubation results in a 30% increase in initial activity of CODH, suggesting that those $[FeNi]^{n+}$ species which disappear upon CO preincubation are "unready" forms. The spectroscopic features of phenosafranin-poised CODH indicate that the putative "unready" forms of the [FeNi] cluster probably have lower reduction potentials than the "ready" forms. EPR-monitored dye-mediated redox titrations are planned to address this issue. Finally, CO is produced from the described system, eliminating the possibility that CO_2 is simply binding to CODH to produce the $g = 1.75$ feature. Elimination of the above possibilities means that only $[(CO_L)\text{-}Fe^{2+}\text{-}Ni^{2+}]^{4+}$ ($S = 1$) coupling with $[Fe_4S_4]_C^{1+}$ ($S = 1/2$) and resulting in the perturbation of the ($S = 1/2$) $[Fe_4S_4]_C^{1+}$ signal remains. The exact nature of this coupling is unknown, but given the proposed coupling scheme for C_{red1}, antiferromagnetic exchange coupling to produce $S_{tot} = |1 - 1/2| = 1/2$ is a possibility. This proposed coupling scheme is very similar to that proposed previously as an explanation for C_{red1}, i.e., the weak exchange coupling of Ni^{2+} ($S = 1$) with $[Fe_4S_4]_C$ ($S = 1/2$).[1]

Assignments of the C_{red} States Are Consistent with Reported Spectroscopy of CODH. Spectroscopic data presented in the literature of CODH poised in states producing C_{red1} and C_{red2} support the assignments given above. Electron−nuclear double resonance (ENDOR) results are consistent with our assignments even though reported measurements were performed on primarily $[Fe_4S_4]$ resonances. The C_{red1} state of *C. thermoaceticum* CODH was shown to have a strongly coupled exchangeable proton, termed H_s.[29] We propose that the C_{red1} state of *R. rubrum* CODH arises from the coupling of the putative $[(CO_L)Fe^{3+}Ni^{2+}\text{-}H^-]^{4+}$ cluster ($S = 1/2$) with $[Fe_4S_4]_C^{1+}$ ($S = 1/2$). Therefore, the strongly coupled proton observed in ENDOR may arise from the hydride atom on the [FeNi] cluster. The literature reports that in the C_{red2} state this strongly coupled proton is lost. This is also consistent with our assignments, as in the C_{red2A} state the [FeNi] cluster is diamagnetic, and in the C_{red2B} state there is no bound hydrogen atom at the [FeNi] cluster. Whereas direct coordination of a hydrogen species to the paramagnetic atom of the putative [FeNi] cluster should be expected to produce hyperfine coupling of several hundred megahertz, the $A_{max}(^1H_s)$ was determined to be 16 MHz for the C_{red1} state of *C. thermoaceticum* CODH. Only a 10−20 MHz hyperfine interaction was observed between the Ni−C species of *D. gigas* hydrogenase and its exchangeable protons, prompting the authors to suggest that the H species is bound to Ni ligands or the Fe atom of the [FeNi] cluster.[21] Therefore, by analogy, as Fe is proposed to be the paramagnetic atom of the [FeNi] cluster of CODH in the C_{red1} state, it is consistent that the putative hydride be bound to the Ni. However, the true hyperfine interaction at the [FeNi] cluster might prove to be much greater than 16 MHz once ENDOR experiments are performed on primarily [FeNi] g-values (e.g. the $g_{ave} = 2.16$ signal) rather than $[Fe_4S_4]$ g-values. The same ENDOR study[29] revealed the presence of strongly coupled ^{14}N resonances in both the C_{red1} and C_{red2} states of *C. thermoaceticum* CODH.

(29) DeRose, V. J.; Telser, J.; Anderson, M. E.; Lindahl, P. A.; Hoffman, B. M. *J. Am. Chem. Soc.* **1998**, *120*, 8767−87776.

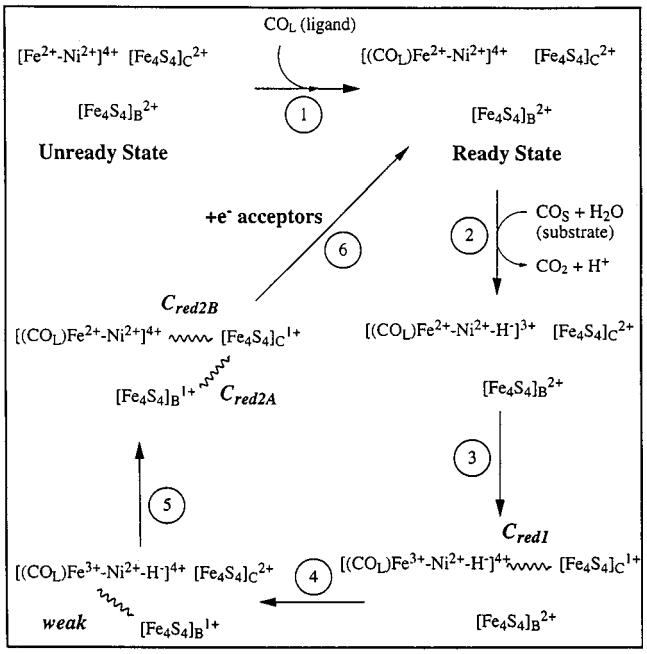

Figure 9. A proposed mechanism for CODH, showing relevant EPR species. The wavy line indicates spin−spin interaction. EPR signals are represented by bold italic font. The term "weak" indicates a weak spin−spin interaction. CO_L stands for a nonsubstrate CO ligand to the [FeNi] cluster. CO_S stands for a substrate CO molecule.

Part 1 in this series provides evidence for hyperfine splitting of the $g_{ave} = 2.16$ signal, possibly by an ^{14}N nucleus. Our assignments predict that both the C_{red1} and C_{red2B} states (not the C_{red2A} state) may have a strongly coupled ^{14}N nucleus due to the paramagnetic states of the [FeNi] cluster ($S = 1/2$ and 1, respectively).

Ni-edge X-ray absorption spectroscopy (XAS) and extended X-ray absorption fine structure (EXAFS) suggest that the Ni redox state does not change significantly in *R. rubrum* CODH in going from oxidized to reduced enzyme.[30] Ni was suggested to remain in the Ni^{2+} oxidation state. These observations are consistent with our assignment that the Fe atom of the putative $[(CO_L)FeNi]$ cluster is redox active, and the other electron sink is a hydrogen (hydride) atom bound to the Ni atom. Interestingly, the Ni-edge XAS of the SI, C, and R forms of the [FeNi] cluster of hydrogenases also suggested that the redox changes responsible for these states did not involve significant changes in electron density at the Ni atom,[31] although it is obvious that redox changes are occurring at the [FeNi] cluster site.

Mechanism of CO Oxidation Incorporating the Proposed Enzyme States Producing the C_{red} Signals. Based upon the above assignments of the EPR signals observed in CODH, a mechanism is proposed for a single turnover of CODH as shown in Figure 9, with the corresponding EPR signals indicated and the steps numbered. In the starting (oxidized) state, CODH is proposed to be present in both "unready" and "ready" states, depending upon handling. As discussed above, the "unready" state can be transformed into the "ready" state (shown in Figure 9 as step 1) by preincubation with CO. This transformation is proposed to involve the binding of a nonsubstrate, but activating,

(30) Tan, G. O.; Ensign, S. A.; Ciurli, S.; Scott, M. J.; Hedman, B.; Holm, R. H.; Ludden, P. W.; Korszun, Z. R.; Stephens, P. J.; Hodgson, K. O. *Proc. Natl. Acad. Sci. U.S.A.* **1992**, *89*, 4427−4431.

(31) Gu, Z.; Dong, J.; Allan, C. B.; Choudhury, S. B.; Franco, R.; Moura, J. J. G.; Moura, I.; LeGall, J.; Przybyla, A. E.; Roseboom, W.; Albracht, S. P. J.; Axley, M. J.; Scott, R. A.; Maroney, M. J. *J. Am. Chem. Soc.* **1996**, *118*, 11155−11165.

CO molecule (CO_L) to the [FeNi] cluster described in Part 1. The "ready" and "unready" states are isoelectronic. In step 2, CO_S (substrate) binds to the $[(CO_L)Fe^{2+}\text{-}Ni^{2+}]^{4+}$ cluster and is transformed to CO_2 in a process of unknown specific mechanism, but possibly in a process similar to a water-gas shift reaction.[32] The $[(CO_L)Fe^{2+}\text{-}Ni^{2+}]^{4+}$ cluster receives the reducing equivalents to yield a $[(CO_L)Fe^{2+}\text{-}Ni^{2+}\text{-}H^-]^{3+}$ ($S = 0$) redox state. In step 3, one electron is transferred to $[Fe_4S_4]_C$ from the Fe of the binuclear cluster, producing the coupling of the resultant $[(CO_L)Fe^{3+}\text{-}Ni^{2+}\text{-}H^-]^{4+}$ ($S = 1/2$) and $[Fe_4S_4]_C^{1+}$ ($S = 1/2$) species to yield C_{red1}. $[Fe_4S_4]_B$ remains oxidized. In step 4, we propose $[Fe_4S_4]_C$ transfers one electron to $[Fe_4S_4]_B$, resulting in a system comprised of $[(CO_L)Fe^{3+}\text{-}Ni^{2+}\text{-}H^-]^{4+}$, $[Fe_4S_4]_C2+$, and $[Fe_4S_4]_B^{1+}$. During step 4, $[Fe_4S_4]_C$ must physically uncouple from the $[(CO_L)FeNi]$ cluster to allow for a drop in reduction potential of $[Fe_4S_4]_C$ such that transfer of electrons from $[Fe_4S_4]_C$ to $[Fe_4S_4]_B$ is possible. Experiments to address the possible physical uncoupling are in progress. EPR spectral data suggest that the spin-interaction of $[(CO_L)Fe^{3+}\text{-}Ni^{2+}\text{-}H^-]^{4+}$ ($S = 1/2$) with $[Fe_4S_4]_B^{1+}$ ($S = 1/2$) is much weaker than that with $[Fe_4S_4]_C^{1+}$ ($S = 1/2$), but may occur (see Part 1). In step 5, the second electron is transferred from the $[(CO_L)\text{-}Fe^{3+}\text{-}Ni^{2+}\text{-}H^-]^{4+}$ cluster to $[Fe_4S_4]_C^{2+}$. The $[(CO_L)Fe^{2+}\text{-}Ni^{2+}]^{4+}/[(CO_L)Fe^{3+}\text{-}Ni^{2+}\text{-}H^-]^{4+}$ "couple" must therefore be near the potential of the $[Fe_4S_4]_C^{2+/1+}$ couple such that the electron transfer is possible. Thus, step 5 may involve the physical recoupling of the $[(CO_L)FeNi]$ cluster with $[Fe_4S_4]_C$, or ligation or conformational changes in the $[(CO_L)FeNi]$ or $[Fe_4S_4]_C$ clusters such that the above condition is met. It is also possible that a proton must be lost from the [FeNi] cluster prior to electron transfer. The resulting system is described as $[(CO_L)\text{-}Fe^{2+}\text{-}Ni^{2+}]^{4+}$ ($S = 1$), $[Fe_4S_4]_C^{1+}$ ($S = 1/2$), $[Fe_4S_4]_B^{1+}$ ($S = 1/2$). The coupled signal most easily observable by EPR in this redox state is C_{red2B} ($g_x = 1.75$), which is proposed to arise from the coupling of $[(CO_L)Fe^{2+}\text{-}Ni^{2+}]^{4+}$ ($S = 1$) with $[Fe_4S_4]_C$ ($S = 1/2$), perturbing the line shape of $[Fe_4S_4]_C^{1+}$. $[Fe_4S_4]_C^{1+}$ ($S = 1/2$) and $[Fe_4S_4]_B^{1+}$ ($S = 1/2$) also couple to produce C_{red2A}, but this signal is swamped by C_{red2B}. The presence of external electron acceptors in the system in step 6 allows for turnover and encompasses several different electron-transfer events.

This proposed mechanism elucidates why CO-titrated CODH in the absence of electron acceptors appears different from dithionite-treated CODH in many reports. In the former case, when CO is not in very large excess, the enzyme turns over one time, and then remains in the following equilibrium:

$$CO_S + H_2O + [(CO_L)Fe^{2+}\text{-}Ni^{2+}]^{4+} + [Fe_4S_4]_C^{1+} + [Fe_4S_4]_B^{1+} \rightleftarrows CO_2 + 2H^+ + [(CO_L)Fe^{2+}\text{-}Ni^{2+}\text{-}H^-]^{3+} + [Fe_4S_4]_C^{1+} + [Fe_4S_4]_B^{1+}$$

$[(CO_L)Fe^{2+}\text{-}Ni^{2+}]^{4+}$ will couple with $[Fe_4S_4]_C^{1+}$ to yield C_{red2B}. C_{red2B} has a similar line shape to the $[Fe_4S_4]_C$ component of C_{red1}, and the intensity of the $g = 1.75$ feature is greater than it is in C_{red2A} caused by coupling of $[Fe_4S_4]_C^{1+}$ and $[Fe_4S_4]_B^{1+}$. Thus, as discussed earlier, the presence of C_{red2B} precludes observation of C_{red2A}. A different situation is present in dithionite-treated samples of CODH. Here, all species are reduced, resulting in $[Fe_4S_4]_B^{1+}$, $[Fe_4S_4]_C^{1+}$, and predominantly $[(CO_L)Fe^{2+}\text{-}Ni^{2+}\text{-}H^-]^{3+}$. $[Fe_4S_4]_B^{1+}$ and $[Fe_4S_4]_C^{1+}$ couple, producing C_{red2A}. $[(CO_L)Fe^{2+}\text{-}Ni^{2+}\text{-}H^-]^{3+}$ is diamagnetic, and cannot spin-couple, allowing C_{red2A} to be observed in a sample-dependent manner. In cases of a very large excess of CO in the absence of electron acceptors, the above equilibrium is pushed toward $[(CO_L)Fe^{2+}\text{-}Ni^{2+}\text{-}H^-]^{2+}$, and the EPR spectrum is almost identical with dithionite-treated CODH.

The mechanism in Figure 9 is by no means complete. As mentioned above, issues which remain to be addressed include the possibility of ligation or structural changes to allow for reduction of $[Fe_4S_4]_B^{2+}$ by $[Fe_4S_4]_C^{1+}$ and subsequent rereduction of $[Fe_4S_4]_C^{2+}$ by $[(CO_L)Fe^{3+}\text{-}Ni^{2+}\text{-}H^+]^{3+}$. This would almost unquestionably mean uncoupling $[Fe_4S_4]_C^{1+}$ from $[(CO_L)\text{-}Fe^{3+}\text{-}Ni^{2+}\text{-}H^-]^{4+}$ and lowering the reduction potential of the $[Fe_4S_4]_C^{2+/1+}$ couple, but will probably also involve changing the redox potential of the [FeNi] cluster and perhaps ligation of the [FeNi] cluster and $[Fe_4S_4]_C$. Additionally, we favor the existence of a ligand bridge from the [FeNi] cluster to $[Fe_4S_4]_C$. Histidine is a possible component of the bridge based upon ENDOR studies of *C. thermoaceticum* CODH [29] and spectral and biochemical properties of the *R. rubrum* H265V CODH variant,[33] but the bridging residue(s) remain unknown. The A-site (or A-cluster) NiFeS clusters of ACS/CODH enzymes have similarities to the C-site of CODH. Furthermore, the sequences of the α and β subunits which contain the A- and C-sites, respectively, have regions of similarity. It seems reasonable to suggest that the A-site might also contain a [FeNi] cluster. This would explain the observation of a diamagnetic $[Fe_4S_4]^{2+}$ cluster in the Mössbauer spectrum, while a paramagnetic NiFeC signal is observed by EPR spectroscopy.[2] The proposed mechanism in this manuscript is based on analyses of the *R. rubrum* enzyme at equilibrium at defined redox potentials. Among the studies remaining to be done are detailed kinetic analyses of this enzyme such as those performed by Seravalli et al. with the *C. thermoaceticum* CODH.[8]

Acknowledgment. We thank Dr. George Reed and Dr. Perry Frey at the Institute for Enzyme Research for use of their EPR facility. We thank Dr. Chris Felix and Dr. William Antholine for use of the multifrequency EPR facility at the Medical College of Wisconsin. We thank Dr. Eckard Münck, Dr. Stephen Ragsdale, and Dr. Javier Seravalli for insightful comments and critical discussions. We are grateful to the reviewers for many useful and insightful comments and suggestions. We thank Dr. Robert L. Kerby and Dr. Gary P. Roberts for many useful discussions and suggestions. This work was supported in part by DOE Basic Energy Sciences Grant DE-FG02-87ER13691 (to P.W.L.) and National Institutes of Health Grant 1 F32 GM 19716-01 (to C.R.S.).

JA990397A

(32) Cotton, F. A.; Wilkinson, G. *Advanced Inorganic Chemistry*, 5th ed.; John Wiley & Sons: New York, 1988.

(33) Spangler, N. J.; Meyers, M. R.; Gierke, K. L.; Kerby, R. L.; Roberts, G. P.; Ludden, P. W. *J. Biol. Chem.* **1998**, *273*, 4059−4064.

(34) The program DDPOWJE was used (available from Dr. Joshua Telser) which solves by matrix diagonalization (EISPACK subroutines) the spin Hamiltonian for a system of two coupled electronic spins, including single ion electronic parameters (*D*, *g* matrices) and isotropic exchange and dipolar coupling. The eigenvalues provide the transition energies and the eigenvectors the transition probabilities. The *g* matrix of one spin (here the $[Fe_4S_4]_C$ cluster) is the frame of reference and the relative orientation of the second spin (here the [FeNi] site) can be varied with respect to this frame using Euler angles. Such a variation in orientation was successfully used by Guigliarelli et al., and was also explored here.[22]